

FINITE-GAP SOLUTIONS OF THE VORTEX FILAMENT EQUATION: ISOPERIODIC DEFORMATIONS

A. CALINI AND T. IVEY

ABSTRACT. We study the topology of quasiperiodic solutions of the vortex filament equation in a neighborhood of multiply covered circles. We construct these solutions by means of a sequence of isoperiodic deformations, at each step of which a real double point is “unpinched” to produce a new pair of branch points and therefore a solution of higher genus. We prove that every step in this process corresponds to a cabling operation on the previous curve, and we provide a labelling scheme that matches the deformation data with the knot type of the resulting filament.

1. INTRODUCTION

In this sequel to [6], we continue our study of the role of integrability for periodic solutions of the Vortex Filament Equation (also known as Localized Induction Equation)

$$\frac{\partial \gamma}{\partial t} = \frac{\partial \gamma}{\partial x} \times \frac{\partial^2 \gamma}{\partial x^2}, \quad (1)$$

a model of the self-induced dynamics of a vortex line in a Eulerian fluid, described in terms of the evolution of the position vector $\gamma(x, t)$ of a space curve parametrized by arclength x .

Hasimoto’s transformation [16]

$$q = \frac{1}{2} \kappa \exp \left(i \int \tau \, ds \right), \quad (2)$$

given in terms of the curvature κ and torsion τ of γ , maps the Vortex Filament Equation (VFE) to the focussing cubic nonlinear Schrödinger (NLS) equation

$$i q_t + q_{xx} + 2|q|^2 q = 0, \quad (3)$$

with the NLS potential q defined up to multiplication by an arbitrary constant phase factor. The integrability of the NLS equation [12, 32] implies that the VFE inherits many of the properties of the integrable equation, including a family of global geometric invariants (conserved quantities) [22], a bihamiltonian structure [3, 22, 27, 29], and special solutions: solitons, finite-gap solutions, and their homoclinic orbits [4, 6, 8, 30].

Periodic boundary conditions for the VFE give rise to closed curves; of those, the class of vortex filaments corresponding to periodic and quasi-periodic finite-gap NLS potentials provides contains striking examples of curves exhibiting special geometric features (such as symmetry and periodic planarity) and interesting topology. Our previous article [6] focused on characterizing geometric properties of finite-gap VFE solutions such as closure, symmetries, self-intersection, and planarity in terms of the Floquet spectrum of associated finite-gap NLS potentials. In contrast, the current work concerns the topological information contained

Date: July 10, 2021.

The authors were partially funded by NSF grants DMS-0204557 and DMS-0608587.

in the algebro-geometric data of a closed VFE solution associated with a periodic finite-gap NLS potential.

Before describing our approach to this problem, we will briefly introduce some of the main tools and results used in the paper.

The NLS linear system and the curve reconstruction formula. The AKNS linear system for (3) consists of a pair of first-order linear systems [12]: an eigenvalue problem

$$\mathcal{L}_1\phi = \lambda\phi, \quad (4)$$

and an evolution equation

$$\phi_t = \mathcal{L}_2\phi \quad (5)$$

for the complex vector-valued eigenfunction ϕ . The solvability or “zero curvature” condition of the AKNS system is the NLS equation (3). Expressed in terms of the Pauli matrix

$$\sigma_3 = \begin{pmatrix} 1 & 0 \\ 0 & -1 \end{pmatrix},$$

$$\mathcal{L}_1 = i\sigma_3 \frac{\partial}{\partial x} + \begin{pmatrix} 0 & q \\ -\bar{q} & 0 \end{pmatrix}, \quad \mathcal{L}_2 = i(|q|^2 - 2\lambda^2)\sigma_3 + \begin{pmatrix} 0 & 2i\lambda q - q_x \\ 2i\lambda\bar{q} + \bar{q}_x & 0 \end{pmatrix}.$$

The coefficients of the linear operators \mathcal{L}_1 and \mathcal{L}_2 depend on x and t through the complex-valued function q , and on the *spectral parameter* $\lambda \in \mathbb{C}$.

The inverse of the Hasimoto map (i.e., the reconstruction of a curve given its curvature and torsion) is realized in terms of the solutions of the AKNS system (equivalent to the Darboux equations for the natural frame of the curve). Remarkably, the reconstruction of the evolving filament requires taking no antiderivatives: given a fundamental matrix solution $\Phi(x, t; \lambda)$ of the AKNS system, such that $\Phi(0, 0; \lambda)$ is a fixed element of $SU(2)$, then the skew-hermitian matrix

$$\gamma(x, t) = \Phi^{-1} \frac{d\Phi}{d\lambda} \Big|_{\lambda=0} \quad (6)$$

satisfies the VFE (1), and corresponds to q via the Hasimoto map [26, 29]. (We have identified $\mathfrak{su}(2)$ with \mathbb{R}^3 via a fixed isometry, under which the Lie bracket corresponds to -2 times the cross product.) Formula (6), known as the *Sym-Pohlmeyer reconstruction formula*, can also be evaluated at a nonzero real eigenvalue $\lambda = \Lambda_0$. The resulting curve γ still satisfies (1), but with a potential that differs from what we started with by the Galilean transformation $q(x, t) \mapsto e^{i(ax - a^2t)}q(x - 2at, t)$, $a = -2\Lambda_0$, which preserves solutions of (3). Given a closed curve of length L , the potential q obtained by the Hasimoto map (2) is not necessarily L -periodic, but will be related to an L -periodic potential by a Galilean transformation. The closed curve may then be recovered using (6), but evaluated at $\lambda = \Lambda_0$.

The Floquet spectrum of a finite-gap solution. The spectrum associated with an L -periodic NLS potential $q(x)$ is defined in terms of the *Floquet discriminant*

$$\Delta(q; \lambda) = \text{Trace}(\Phi(x + L, t; \lambda)\Phi(x, t; \lambda)^{-1}),$$

the trace of the transfer matrix across one period L , where Φ is a fundamental matrix solution of the AKNS system. The Floquet spectrum is the set of complex λ values for which the eigenfunctions of the AKNS system are bounded on the spatial domain:

$$\sigma(q) = \{\lambda \in \mathbb{C} \mid \Delta(q; \lambda) \in \mathbb{R}, -2 \leq \Delta \leq 2\}.$$

It can be shown that Δ is a conserved functional of the NLS time evolution, and in fact a generating function of the constants of motion. In particular, the spectrum of a given NLS potential is invariant under the evolution.

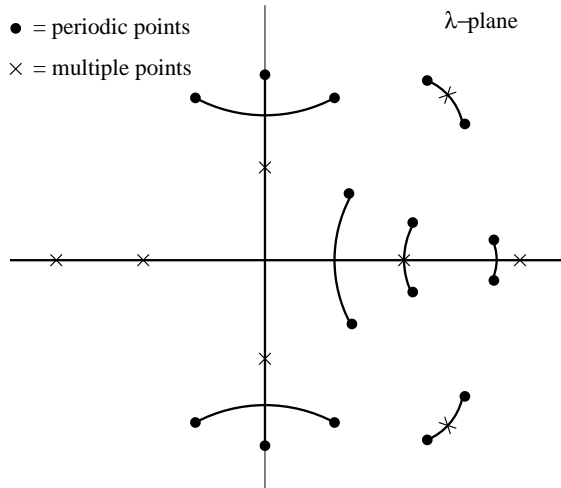


FIGURE 1. The Floquet spectrum of a finite-gap NLS potential.

In Figure 1, we show a typical spectrum for a finite-gap potential, which has a finite number of complex bands of continuous spectrum. Those points at which $\Delta = \pm 2$ are divided into *simple points* and *multiple points*, according to their multiplicity as zeros of $\Delta^2 - 4$. (Finite-gap potentials are characterized by having a finite number of simple points.) Multiple points are among the *critical points* for Δ ; for example, double points satisfy $d\Delta/d\lambda = 0$, but $d^2\Delta/d\lambda^2 \neq 0$. Real double points are removable [28], i.e., at these λ -values the transfer matrix has a pair of linearly independent eigenvectors.

Critical points where Δ does not achieve its maximum or minimum value are embedded within bands of continuous spectrum. It can be easily shown that $d\Delta/d\lambda = 0$ at transverse intersections of bands of continuous spectrum. Those critical points associated with spines intersecting the real axis play an important role in the closure condition of the reconstructed curve, as well as in our analysis.

The quasi-momentum differential and the closure condition. At a generic complex λ , the transfer matrix has a pair of distinct eigenvalues $\rho^+(\lambda)$, $\rho^-(\lambda)$ known as *Floquet multipliers*. The relation between Floquet multipliers and Floquet discriminant is given by

$$\rho^\pm(\lambda) = \frac{\Delta(\lambda) \pm \sqrt{\Delta(\lambda)^2 - 4}}{2}.$$

Thus, $\rho^\pm(\lambda)$ are branches of a holomorphic function ρ which is well defined on a two-sheeted Riemann surface Σ , whose projection $\pi : \Sigma \rightarrow \mathbb{C}$ is branched at the simple points. For $P \in \Sigma$, we will let

$$\rho(P) = e^{iL\Omega_1(P)},$$

where the function $\Omega_1(P)$ is defined up to adding an integer multiple of $2\pi/L$. Its differential

$$d\Omega_1 = \frac{1}{iL} d \log \rho,$$

known as the *quasimomentum differential*, is a well-defined meromorphic differential on Σ . Because $d\Omega_1$ changes by minus one from sheet to sheet, each pair of its zeros projects to a single λ -value, and we will regard its zeros as being located in the complex plane.

For a given finite-gap NLS potential, the real zeros of $d\Omega_1$ (which are the real critical points) play a role in the following result by Grinevich and Schmidt [15]:

Closure Conditions. *A finite-gap VFE solution γ obtained from the generalized Sym-Pohlmeyer reconstruction formula (6) at $\lambda = \Lambda_0$ is smoothly closed if the reconstruction point Λ_0 is (i) a real double point and (ii) a zero of the quasimomentum differential.*

(See also [6] for a derivation of the closure conditions from the explicit formulas for finite-gap VFE solutions.)

Closure conditions must of course be satisfied if one is interested in establishing connections between the knot types of closed finite-gap VFE solutions and the spectra of the associated NLS potentials. However, such conditions turn out to be difficult to compute, as they involve solving implicit equations written in terms of hyperelliptic integrals.

The central idea of this paper is to approach the problem of constructing closed finite-gap solutions of the VFE by starting with an already closed curve of particularly simple type (namely a multiply covered circle) and deforming its associated spectrum in such a way that both periodicity of the corresponding NLS potential and closure of the curve are preserved. By iterating similar isoperiodic deformation steps, we construct a neighborhood of the initial curve that consists of closed finite-gap solution of increasing complexity. (Indeed, at each step of the deformation, a real double point is “opened up” into a new pair of branch points, thus increasing the genus of the Riemann surface by one.)

A beautiful consequence of this multi-step construction is a *labelling scheme* that matches the deformation data with the knot type of the resulting filament. Our main result, the Cabling Theorem (Theorem 5.1) is that every step in this process is, from the topological point of view, a cabling operation on the previous curve, with the cabling type encoded in which real double points are selected to be deformed into a new pair of branch points. A simplified statement of this result is:

Cabling Theorem. *Given relatively prime integers n, m_1, \dots, m_K such that $|m_k| > n > 1$, let $g_k = \gcd(n, m_1, \dots, m_k)$ for $1 \leq k \leq K$. Then there exist a sequence of deformations (i.e., one-parameter families) of finite-gap potentials $q^{(k)}(x; \epsilon)$ of fixed period L , and complex numbers $\Lambda_0^{(k)}(\epsilon)$, which are both analytic in ϵ , such that*

- (1) $q^{(k)}$ is of genus k when $\epsilon \neq 0$, $q^{(k)}(x; 0) = q^{(k-1)}(x, \epsilon_{k-1})$ for some $\epsilon_{k-1} > 0$ when $k > 1$, and $q^{(1)}(x; 0)$ is constant;
- (2) the filament $\gamma^{(k)}(x; \epsilon)$ that is constructed from $q^{(k)}(x; \epsilon)$ using the Sym-Pohlmeyer formula evaluated at $\Lambda_0^{(k)}(\epsilon)$ is closed of length $n\pi/g_k$ and is, for ϵ sufficiently small, a $(g_{k-1}/g_k, m_k/g_k)$ -cable about $\gamma^{(k)}(x; \epsilon_{k-1})$.

The full statement of Theorem 5.1 explains how these deformations arise from isoperiodic deformations of the spectrum, and how the data $[n, m_1, \dots, m_K]$ determine the selection of double points to be opened up. From an argument in the proof of Theorem 5.1, we deduce as a bonus that the knot types of the finite-gap filaments so constructed are constant under the VFE evolution (see Corollary 5.2), ultimately confirming and justifying the use of the Floquet spectrum as a tool for classifying the knot types of closed curves in an appropriate neighborhood of multiply covered circles. (In fact, such curves are approximated by finite-gap solutions that are dense in the space of periodic solutions of the VFE [13].)

The proof of the main result brings together a variety of tools from the periodic theory of integrable systems and the perturbation theory of ordinary differential equations. We mention them below while giving a brief description of the paper contents and organization.

Section 2 contains the motivation of this work and the framework of our approach. After introducing Grinevich and Schmidt's isoperiodic deformation system, we define a special type of closure-preserving isoperiodic deformation that reverses "pinching" of the two ends of a spine of spectrum into a real double point (homotopic deformations), and show that the solution to such a deformation is analytic in the deformation parameter. We then proceed to deform off the spectrum of a modulationally unstable plane wave solution (corresponding to a multiply-covered circle solution of the VFE), and compute the spatial frequencies of the resulting finite-gap solutions. Examples of the curves resulting from successive homotopic deformations, and a labelling scheme for their knot types are presented in Section 3. Section 4 makes use of the completeness of the family of squared eigenfunctions for the AKNS system to characterize, to first order, the perturbations of the potential q associated with homotopic deformations. The Cabling Theorem and its proof are the contents of Section 5: the proof is a combination of explicit perturbative computations involving the squared eigenfunctions, a topological argument based on White's formula for self-linking, and a careful analysis of the argument of the first order correction to the initial potential, which determines the cabling phenomenon and the cable type. The two appendices (Sections 6 and 7) contain a statement of the completeness theorem for squared eigenfunctions and related useful results, and a proof of the analytic dependence of the potential q on the deformation parameter.

2. ISOPERIODIC DEFORMATIONS

Inspecting the formula (36) for a finite-gap NLS solution $q(x, t)$ shows that q is periodic in x if and only if the components of the frequency vector $\mathbf{V} \in \mathbb{R}^g$ and a real scalar E are rationally related. These data are determined by a choice of $g + 1$ pairs of conjugate branch points in the complex plane. Furthermore, because E changes additively when the branch points are translated in the real direction, construction of a periodic solution depends on being able to select the components V_j of the frequency vector. We now describe a scheme for deforming the spectrum of a multiply-covered circle which produces arbitrary rational values for these components.

Grinevich and Schmidt [14] developed a method for deforming the branch points in a way that preserves the components V_k of the frequency vector. Such isoperiodic deformations of the spectrum were first introduced by Krichever [21] in connection with topological quantum field theory, and are naturally related to the Whitham equations in the work of Flaschka, Forest and McLaughlin [10]. Although the zeros $\alpha_1, \dots, \alpha_{g+1}$ of the quasimomentum differential $d\Omega_1$ are dependent on the branch points $\lambda_1, \dots, \lambda_{2g+2}$, when we incorporate these α_k as dependent variables the isoperiodic deformation becomes a system of ordinary differential equations with rational right-hand sides:

$$\begin{aligned} \frac{d\lambda_j}{d\xi} &= - \sum_{k=1}^{g+1} \frac{c_k}{\lambda_j - \alpha_k} \quad 1 \leq j \leq 2g + 2, \\ \frac{d\alpha_k}{d\xi} &= \sum_{\ell \neq k} \frac{c_k + c_\ell}{\alpha_\ell - \alpha_k} - \frac{1}{2} \sum_{j=1}^{2g+2} \frac{c_k}{\lambda_j - \alpha_k}, \quad 1 \leq k, \ell \leq g + 1. \end{aligned} \tag{7}$$

Here, c_1, \dots, c_{g+1} are controls, i.e., arbitrary functions of the real deformation parameter ξ . In the case of finite-gap NLS solutions, the λ_j and α_k are roots of a real polynomial, and it is easily checked that complex conjugacy relationships among these roots (e.g., $\lambda_{2j+2} = \overline{\lambda_{2j+1}}$, $\alpha_2 = \overline{\alpha_1}$, $\alpha_3 = \overline{\alpha_3}$) are preserved by these deformations, provided that the controls c_k have the same conjugacy relationships as the α_k .

The change in the value of the quasimomentum Ω_1 at one of the α_k under this deformation is given by

$$\frac{d}{d\xi}\Omega_1(\alpha_k) = c_k \left(\frac{1}{\lambda - \alpha_k} \frac{d\Omega_1}{d\lambda} \right) \Big|_{\lambda=\alpha_k}.$$

Thus, we may preserve the value of $\Omega_1(\alpha_k)$ simply by setting c_k to zero. In particular, if α_k is real and the value of $\Omega_1(\alpha_k)$ is such that the Sym-Pohlmeyer reconstruction formula (6) yields a closed curve at $\Lambda_0 = \lambda_k$, then by choosing the control $c_k = 0$ the isoperiodic deformation will produce a closed curve for every ξ . We will refer to this specialization of isoperiodic deformations as a *homotopic deformation*, since it generates a homotopy through the family of smooth maps of the circle into \mathbb{R}^3 .

Instances of homotopic deformation have been observed before. David Singer and the second author [17] constructed one-parameter families of closed elastic rod centerlines (which correspond to genus one finite-gap NLS solutions under the Hasimoto map) in the form of torus knots, terminating in multiply-covered circles at either end of the deformation. We can try to generate this deformation using system (7) with $g = 1$. Assume that, say, α_2 is the real critical point that yields a closed curve. (Necessarily, the other critical point α_1 must be real.) Then choosing $c_2 = 0$ and $c_1 = 1$ will reproduce part of this homotopic deformation. The ‘circular’ end of the deformation occurs when α_1 and one of the complex conjugate pairs of branch points (say, λ_1 and $\bar{\lambda}_1$) limit to the same real value as ξ decreases to some finite time T_1 . Note that this is a singularity of the isoperiodic deformation system, as the right-hand side of (7) blows up as $\lambda_1 \rightarrow \alpha_1$. In the next subsection, we will examine this type of singularity for (7) in more detail.

The genus one solution of (7) discussed above also reaches a singularity in finite forward time, when the two α ’s collide. In our previous paper [6] we showed that this other kind of singularity is associated with the elastic rod centerline becoming an Euler elastic curve. Presumably, the solution may be continued smoothly through the singularity, although we have not investigated this question.

2.1. Pinch-Type Singularities. We will say that a solution of (7) (in arbitrary genus) has a *pinch-type singularity* when exactly two complex conjugate branch points and exactly one real critical point α_k approach the same real value. (The reason for the name is that bringing two branch points together collapses a homotopy cycle on the associated Riemann surface, hence pinching one handle on a g -handled torus.) We will limit our attention to the case where only the control associated to α_k is nonzero.

Because the system (7) is invariant under permuting the indices on the branch points, and invariant under simultaneously permuting the indices on the critical points and the controls, we can without loss of generality let λ_1 and $\lambda_2 = \bar{\lambda}_1$ be the colliding branch points, and α_1 the critical point, with $c_1 = 1$ being the only nonzero control. Then the system takes the form

$$\begin{aligned} \frac{d\lambda_j}{d\xi} &= -\frac{1}{\lambda_j - \alpha_1}, & 1 \leq j \leq 2g + 2, \\ \frac{d\alpha_1}{d\xi} &= \sum_{k=2}^{g+1} \frac{1}{\alpha_k - \alpha_1} - \frac{1}{2} \sum_{j=1}^{2g+2} \frac{1}{\lambda_j - \alpha_1}, \\ \frac{d\alpha_k}{d\xi} &= \frac{1}{\alpha_1 - \alpha_k}, & 2 \leq k \leq g + 1. \end{aligned} \tag{8}$$

In particular, because $\lambda_2 = \overline{\lambda_1}$,

$$\frac{d(\lambda_1 - \alpha_1)}{d\xi} = -\frac{1}{2} \left(\frac{1}{\lambda_1 - \alpha_1} - \frac{1}{\overline{\lambda_1} - \alpha_1} \right) + \frac{1}{2} \sum_{j=3}^{2g+2} \frac{1}{\lambda_j - \alpha_1} - \sum_{k=2}^{g+1} \frac{1}{\alpha_k - \alpha_1},$$

showing that, if $\lambda_1 - \alpha_1$ approaches zero as $\xi \searrow 0$, and the other differences $\lambda_j - \alpha_1$ and $\alpha_k - \alpha_1$ have nonzero limits, then $\text{Im}(\lambda_1 - \alpha_1)$ should approach zero like $\sqrt{2\xi}$.

Proposition 2.1. *When the change of variable $\xi = \frac{1}{2}t^2$ is made in (8), the resulting system has a solution which is analytic at $t = 0$ and satisfies*

$$\begin{aligned} \alpha_k &= \alpha_k^0 + O(t^2), & 1 \leq k \leq g+1 \\ \lambda_1 &= \alpha_1^0 + it + O(t^2), \\ \lambda_2 &= \overline{\lambda_1}, \\ \lambda_j &= \lambda_j^0 + O(t^2), & 3 \leq j \leq 2g+2, \end{aligned}$$

where α_1^0 is real, and for $k > 1$ and $j > 2$, the values α_k^0, λ_j^0 are distinct from α_1^0 .

Proof. Let $\lambda_1 - \alpha_1 = x + iy$ and $z = \text{Re}(\lambda_1)$. Then, because α_1 is real,

$$\frac{dz}{d\xi} = -\text{Re} \left(\frac{1}{\lambda_1 - \alpha_1} \right) = \frac{-x}{x^2 + y^2}.$$

Because the remaining α 's are real, and the λ_j are in complex conjugate pairs (with $\lambda_2 = \overline{\lambda_1}$),

$$\begin{aligned} \frac{dy}{d\xi} &= -\text{Im} \left(\frac{1}{\lambda_1 - \alpha_1} + \sum_{k>1} \frac{1}{\alpha_k - \alpha_1} - \frac{1}{2} \sum_j \frac{1}{\lambda_j - \alpha_1} \right) \\ &= -\frac{1}{2} \text{Im} \left(\frac{1}{\lambda_1 - \alpha_1} - \frac{1}{\overline{\lambda_1} - \alpha_1} \right) = \frac{y}{x^2 + y^2}. \end{aligned}$$

and

$$\frac{dx}{d\xi} = -\text{Im} \left(\frac{1}{\lambda_1 - \alpha_1} + \sum_{k>1} \frac{1}{\alpha_k - \alpha_1} - \frac{1}{2} \sum_j \frac{1}{\lambda_j - \alpha_1} \right) = \frac{1}{2} \sum_{j>2} \frac{1}{\lambda_j - \alpha_1} - \sum_{k>1} \frac{1}{\alpha_k - \alpha_1} := N.$$

Note that the quantity N is, by assumption, a nonzero analytic function of its arguments at their initial values $\lambda_j = \lambda_j^0$, $\alpha_1 = \alpha_1^0$, and $\alpha_k = \alpha_k^0$, for $j > 2$ and $k > 1$.

We now change to y as independent variable, and introduce the new dependent variables

$$\tilde{x} = x/y, \quad \tilde{z} = (z - \alpha_1^0)/y, \quad \tilde{\lambda}_j = (\lambda_j - \lambda_j^0)/y, \quad \tilde{\alpha}_k = (\alpha_k - \alpha_k^0)/y.$$

Of course, if the conclusions of the proposition hold, then these new variables will be analytic functions of y that vanish to at least order one when $y = 0$. In terms of these new dependent

and independent variables, the system becomes

$$\begin{aligned} y \frac{d\tilde{x}}{dy} &= -\tilde{x} + y(1 + \tilde{x}^2)N \\ y \frac{d\tilde{z}}{dy} &= -\tilde{x} - \tilde{z}, \\ y \frac{d\tilde{\lambda}_j}{dy} &= -\tilde{\lambda}_j - \frac{y(1 + \tilde{x}^2)}{\lambda_j^0 - \alpha_1^0 + y(\tilde{x} - \tilde{z} + \tilde{\lambda}_j)}, \\ y \frac{d\tilde{\alpha}_k}{dy} &= -\tilde{\alpha}_k - \frac{y(1 + \tilde{x}^2)}{\alpha_k^0 - \alpha_1^0 + y(\tilde{x} - \tilde{z} + \tilde{\alpha}_k)}. \end{aligned}$$

This system has a Briot-Bouquet singularity at the origin. Linearizing the right-hand sides at $\tilde{x} = \tilde{z} = \tilde{\lambda}_j = \tilde{\alpha}_k = 0$ gives a lower-triangular coefficient matrix all of whose eigenvalues are equal to -1 . Thus, there is a unique solution all of whose components vanish when $y = 0$ and which is analytic in y near $y = 0$ (see, for example, p. 21 in [18] or Theorem 59 in [33]¹). Consequently, x, z, λ_j and α_k are analytic functions of y which satisfy

$$x = O(y^2), \quad z = \alpha_1^0 + O(y^2), \quad \lambda_j = \lambda_j^0 + O(y^2), \quad \alpha_k = \alpha_k^0 + O(y^2). \quad (9)$$

Because $d\xi/dy = y(1 + \tilde{x}^2)$, it follows that ξ is an analytic function of y^2 , and we can arrange that $\xi = 0$ when $y = 0$. Then $\xi = \frac{1}{2}y^2 + O(y^4)$. Thus, we can define an analytic function t of y such that $\xi = \frac{1}{2}t^2$ and $t = y + O(y^2)$. Clearly, this function is invertible for $|y|$ sufficiently small, so we may replace y by t in (9), and assert that y is an analytic function of t satisfying $y = t + O(t^2)$. Rewriting these equations in terms of the original variables λ_1 and α_1 completes the proof. \square

Note that the variable t in Proposition 2.1 will be replaced by the more commonly-used deformation parameter ϵ in later sections of this paper.

2.2. Deforming the Multiply-Covered Circle. Our main idea is to use the isoperiodic deformations provided by Proposition 2.1 to create new, higher-genus NLS solutions while maintaining the closure of the filament (in effect, reversing the collapse of branch points described above in the genus one case). By continuity, the initial value α_1^0 used must be a real point of the discrete spectrum (hence, a real double point) of the lower-genus NLS solution. So, when we carry out several deformations in succession, we must keep track of the continuously changing positions of those double points that we want to split later. We can do this by incorporating them as extra variables in (8), consisting of one critical point and a pair of branch points that remain equal as the deformation progresses. (Note that, for example, the equality $\lambda_3 = \lambda_4 = \alpha_2$ is preserved under the deformation (8).)

We will begin the multi-step deformation process by selecting g double points from the spectrum of a multiply-covered circle to be the initial values for $\alpha_1, \dots, \alpha_g$, and begin the deformation by setting $\lambda_{2k} = \lambda_{2k-1} = \alpha_k$ for $1 \leq k \leq g$. (There will be two addition

¹In the sources cited, the results are given for Briot-Bouquet systems $zdy_i/dz = F_i(z, y_1, \dots, y_n)$ where the linearization has k positive eigenvalues, the resulting solution is a double power series in z and $\ln z$ that converges for $|z|$ sufficiently small in a sector about the origin in the complex plane, and the solution depends on k constants. It is implicit in the statements of these results that, when $k = 0$, the solution is unique and analytic in z . In that case, the existence/uniqueness result can also be proved in a more elementary way using the method of majorants.

branch points with initial values $\lambda_{2g+1} = i$ and $\lambda_{2g+2} = -i$, and an additional α_{g+1} initially equal to zero.) The first deformation, which produces a genus one (elastic rod) solution, will be continued up to a small value of the deformation parameter. Then, α_2 replaces α_1 as the initial value for the next double point to be split, and so on until all g double points have been split. Note that we will assume that the amplitude of each deformation step (i.e., the maximum value of ξ attained) is sufficiently small so that singularities are avoided. (Consequently, all critical points remain real.) As we will see in later sections, it is also necessary to assume that the amplitude of each step is small relative to the last one, in order to be able to predict the topological type of the resulting filament.

We will be able to calculate the frequencies V_k for the genus g NLS solution by using the fact that the frequencies are unchanged by isoperiodic deformations, and are determined by the integrals of certain holomorphic differentials around cycles on the Riemann surface. These integrals can, in turn, be calculated by following the sequence of deformations back to the multiply-covered circle, and doing residue calculations using the initial positions of the double points.

We begin this calculation with the spectrum of the multiply-covered circle. Using the Hasimoto map (2), the potential $q(x) \equiv 1$ corresponds to a circle with curvature $\kappa = 2$, radius $1/2$, and length π . A fundamental matrix solution for the spatial part of the NLS linear system

$$\frac{d\phi}{dx} = \begin{bmatrix} -i\lambda & iq \\ i\bar{q} & i\lambda \end{bmatrix} \phi \quad (10)$$

with $q = 1$ is given by

$$\Phi(x; \lambda) = \begin{bmatrix} \cos(\omega x) - \frac{i\lambda}{\omega} \sin(\omega x) & \frac{i}{\omega} \sin(\omega x) \\ \frac{i}{\omega} \sin(\omega x) & \cos(\omega x) + \frac{i\lambda}{\omega} \sin(\omega x) \end{bmatrix}, \quad \omega = \sqrt{1 + \lambda^2}.$$

The periodic spectrum for the singly-covered circle, computed relative to period $L = \pi$, consists of two simple points $\lambda = \pm i$, and infinitely many real double points given by $\lambda = \pm\sqrt{m^2 - 1}$, $m = 1, 2, 3, \dots$ (In fact, the origin is a point of order four.) For the n -times-covered circle we compute the periodic spectrum relative to period $L = n\pi$, and this consists of the same simple points, but with double points given by

$$\lambda = \pm\sqrt{(m/n)^2 - 1}, \quad m = 1, 2, 3, \dots \quad (11)$$

Note that the origin is the only point of the periodic spectrum that can be used as the value Λ_0 producing a closed curve via the Sym-Pohlmeyer reconstruction formula (6). Thus, zero will be one of the initial values for the critical points in the first step of the deformation process, and the corresponding control will always be set to zero in order to maintain closure; we will use Λ_0 to denote this ‘reconstruction point’, which will move along the real axis during the deformation steps.

Let $\beta_1 < \beta_2 < \dots < \beta_g$ denote the choice of double points of the spectrum of the n -times covered circle to be opened up. (For the following calculation, it is not relevant in what order they are opened up.) We will now determine the relationship between these double points and the periods of the genus g solution obtained once all g points have been opened up. According to the construction for finite-gap solutions set forth in [2] and [6], the frequency vector $[V_1, \dots, V_g]$ is $4\pi i$ times the first column of the inverse of the matrix A defined by

$$A_k^j = \int_{a_k} \frac{\lambda^{g-j} d\lambda}{\zeta},$$

where ζ is related to λ by the defining equation of the hyperelliptic curve,

$$\zeta^2 = \prod_{j=1}^{2g+2} (\lambda - \lambda_j),$$

and each cycle a_k circles around (in a clockwise fashion, on the upper sheet²) the pair of complex conjugate branch points into which β_k has been split (see Figure 5).

First, consider the case when all β 's are negative. Then, as we run the deformation steps backward, the cycles a_1, \dots, a_g become loops around β_1, \dots, β_g , and the only remaining branch points are $\pm i$. The denominator ζ in the integrand limits to $-\sqrt{\lambda^2 + 1} \prod_{j=1}^g (\lambda - \beta_j)$ along the a -cycles, taking the square root as positive along the real axis. A residue calculation then gives

$$\lim A_k^j = N_k^j = \frac{2\pi i \beta_k^{g-j}}{\sqrt{\beta_k^2 + 1} \prod_{\ell \neq k} (\beta_k - \beta_\ell)}.$$

(Note that the minus sign in ζ is offset by the clockwise orientation of the a -cycles.) We may factor this matrix as

$$N = 2\pi i \begin{bmatrix} \beta_1^{g-1} & \dots & \beta_g^{g-1} \\ \beta_1^{g-2} & \dots & \beta_g^{g-2} \\ \dots & \dots & \dots \\ 1 & \dots & 1 \end{bmatrix} \begin{bmatrix} 1/D_1 & 0 & \dots & 0 \\ 0 & 1/D_2 & \dots & 0 \\ \dots & \dots & \dots & \dots \\ 0 & 0 & \dots & 1/D_g \end{bmatrix}, \quad D_k = \sqrt{\beta_k^2 + 1} \prod_{\ell \neq k} (\beta_k - \beta_\ell). \quad (12)$$

Its inverse is

$$N^{-1} = \frac{1}{2\pi i} \begin{bmatrix} D_1 & 0 & \dots & 0 \\ 0 & D_2 & \dots & 0 \\ \dots & \dots & \dots & \dots \\ 0 & 0 & \dots & D_g \end{bmatrix} \frac{1}{\prod_{j < k} (\beta_j - \beta_k)} \begin{bmatrix} \prod_{j < k; j, k \neq 1} (\beta_j - \beta_k) & \dots \\ (-1) \prod_{j < k; j, k \neq 2} (\beta_j - \beta_k) & \dots \\ (-1)^2 \prod_{j < k; j, k \neq 3} (\beta_j - \beta_k) & \dots \\ \dots & \dots \end{bmatrix}.$$

(Only the first column is needed for the matrix on the right.) Thus,

$$V_j = 2\sqrt{\beta_j^2 + 1}, \quad 1 \leq j \leq g. \quad (13)$$

Next, suppose that $\beta_1 < \dots < \beta_K < 0 < \beta_{K+1} < \dots < \beta_g$. Because the branch cut between i and $-i$, the roles of upper sheet and lower sheet are switched an extra time, and the residue calculation gives

$$\lim A_k = \begin{cases} N_k, & 1 \leq k \leq K, \\ -N_k, & K+1 \leq k \leq g, \end{cases}$$

where N_k is the k th column of the matrix defined by (12) and A_k is the k th column of matrix A . Solving for $\lim A^{-1}$ gives the following frequency formulas:

$$V_j = \begin{cases} 2\sqrt{\beta_j^2 + 1}, & 1 \leq j \leq K, \\ -2\sqrt{\beta_j^2 + 1}, & K+1 \leq j \leq g \end{cases} \quad (14)$$

²Along the real λ axis, we initially label as the upper sheet that containing the point ∞_+ , where λ^{g+1}/ζ tends to $+1$ as $\lambda \rightarrow +\infty$, but as one proceeds from right to left along the real axis in the λ -plane, the roles of upper sheet and lower sheet are exchanged along branch cuts that run between each branch point and its conjugate, parallel to the imaginary axis.

3. EXAMPLES OF CABLING OPERATIONS

Comparing the frequency formulas (13) and (14) with formula (11) for the spectrum of the multiply-covered circle shows that when the double points β_j are chosen as members of that spectrum, the frequencies attained by the deformations have rational values. Accordingly, we will introduce a notation for these deformations that allows these values to be read off easily.

We will use the notation

$$[n; m_1, \dots, m_g], \quad |m_j| > n$$

to indicate the result of g successive homotopic deformations of the n -times covered circle, opening up the real double points whose starting position is $\beta_j = -\text{sign}(m_j)\sqrt{(m_j/n)^2 - 1}$ in the order in which the m_j appear in the square brackets.³ (The minus sign is incorporated here to compensate for the sign in (14).) As mentioned before, we will assume that the amplitude of each deformation step is small relative to that of the previous step. We will also assume that the numbers in square brackets m_i are relatively prime, so that the double points selected do not all belong to the spectrum of a multiply-covered circle for a smaller value of n . In this notation, it is easy to see that $[n; m]$ gives frequency $V = m/n$, $[n; m_1, m_2]$ gives frequency vector $[m_1/n, m_2/n]$, and so on. These frequencies determine the length of the corresponding filament as follows:

The finite-gap NLS solution $q(x, t)$ takes the form

$$q(x, t) = A \exp(-iEx + iNt)\theta(i\mathbf{V}x + i\mathbf{W}t - \mathbf{D} + \mathbf{r})/\theta(i\mathbf{V}x + i\mathbf{W}t - \mathbf{D}),$$

where A, E, N are constants, \mathbf{V} is the frequency vector, \mathbf{D} and \mathbf{r} are constant vectors in \mathbb{C}^g , and θ is a Riemann theta function with periods that are $2\pi i$ times an integer vector. (For more details, see §7.) The phase factor $\exp(-iEx)$ may be removed by an appropriate gauge transformation of NLS, and then, assuming the components of \mathbf{V} are rational, the period of the potential q is the least common (integer) multiple of the periods $2\pi/V_j$. The Baker-Akheizer functions, quadratic products of which are used to reconstruct the Frenet frame of the filament, take the form

$$\psi_i = C_i(P) \exp(ix\Omega_1(P) + it\Omega_2(P))\theta(i\mathbf{V}x + i\mathbf{W}t + \mathbf{D}_i(P))/\theta(i\mathbf{V}x + i\mathbf{W}t - \mathbf{D}), \quad i = 1, 2,$$

where P a point on the Riemann surface lying over the reconstruction point Λ_0 , $\Omega_{1,2}$ are certain Abelian integrals on Σ , and $C_{1,2}$ and $\mathbf{D}_{1,2}$ are constants that depend on P . Under the homotopic deformation process we have described above, the value $\Omega_1(P)$ is preserved, so can be obtained by calculating its limit as we run the deformation process backwards to the multiply-covered circle. Again, we first calculate this assuming that all the limiting values β_j of the double points are negative. Then, because

$$d\Omega_1 = \frac{\prod_{j=1}^{g+1} (\lambda - \alpha_j)}{\zeta} d\lambda,$$

the limiting value of this differential, on the upper sheet above the origin, is

$$\lim d\Omega_1 = \frac{\lambda d\lambda}{\sqrt{\lambda^2 + 1}}.$$

³However, it matters in which order the deformations are done, for it is easily checked that if \mathbf{v}_j is the vector field on \mathbb{C}^{3g+3} defined by setting $c_j = 1$ and all other controls zero in the system (7), then the vector fields \mathbf{v}_j and \mathbf{v}_k do not commute when $j \neq k$.

Integrating from the limit $-i$ of the basepoint for Ω_1 (which is by convention the point in the lower half-plane not enclosed by the basis a -cycles) to the origin, which is the limit of the reconstruction point, gives $\Omega_1(P) = 1$. Next, assuming that the least positive double point is β_{K+1} ,

$$\lim d\Omega_1 = (-1)^{g-K} \frac{\lambda d\lambda}{\sqrt{\lambda^2 + 1}}.$$

Integrating this from the basepoint to the origin gives $\Omega_1(P) = (-1)^{g-K}$. Thus, the factor $\exp(2ix\Omega_1(P))$, which occurs in quadratic products of Baker functions, has period π . Since this factor is multiplied the theta functions, the period of the Frenet frame is the least common multiple of π and the numbers $2\pi/V_j$ for $1 \leq j \leq g$. Because the reconstruction point is chosen so that the integral of the Frenet unit tangent vector is zero, this period is also the length of the filament.

As we will eventually show, the selection of frequencies determines the knot type of the resulting filament as an iterated cable knot. This can be viewed as a generalization of the work of Keener [19], who showed that if one adds to a circle of length L a small perturbation of period $(n/m)L$, and a closed curve results, then the perturbed circle is a (n, m) torus knot (i.e., it covers the original circle n times lengthwise, and wraps around the circle m times). The Figures 2 through 4 show examples of our iterated cable construction.

4. ISOPERIODIC DEFORMATIONS AND SQUARED EIGENFUNCTIONS

In this section we show how, for an NLS solution q_0 of a given period, the only isoperiodic deformations that preserve the reality condition $r = -\bar{q}$ (see §6 for notation) and open up just one real double point λ_0 , while leaving all other points of the discrete spectrum and the critical points unchanged at first order, must be linear combinations with real coefficients of $(\varphi^+)_1^2 + (\bar{\varphi}_2^+)^2$ and $i[(\varphi^+)_1^2 - (\bar{\varphi}_2^+)^2]$, written in terms of the components of a Bloch eigenfunction φ^+ evaluated at λ_0 . The proof requires computing the first order variations of the discrete spectrum (simple and multiple points) and of the critical points. For the purpose of this paper, it is sufficient to discuss the computation of the first order variation of a real double point; the cases of simple and critical points can be treated analogously.

Assume that $(q_0 + \epsilon q_1, r_0 + \epsilon r_1)$ is a periodic perturbation of a NLS potential $\mathbf{q}_0 = (q_0, r_0)$ of a fixed period L , and assume that the pair (ϕ_0, λ_0) solves the AKNS eigenvalue problem at \mathbf{q}_0 , where λ_0 is a real double point in the spectrum of the unperturbed potential \mathbf{q}_0 . Let $\phi = \phi_0 + \epsilon \phi_1$ and $\lambda = \lambda_0 + \epsilon \lambda_1$ be the corresponding variations of eigenfunction and eigenvalue. At first order in ϵ , we obtain

$$\mathcal{L}_1 \phi_1 = \begin{pmatrix} -i\lambda_1 & iq_1 \\ -ir_1 & i\lambda_1 \end{pmatrix} \phi_0, \quad (15)$$

where $\mathcal{L}_1 = \frac{d}{dx} - \begin{pmatrix} -i\lambda_0 & iq_0 \\ -ir_0 & i\lambda_0 \end{pmatrix}$ is the spatial operator of the unperturbed AKNS linear system at λ_0 .

Together with the homogeneous linear system $\mathcal{L}_1 \phi_0 = \mathbf{0}$, we consider its formal adjoint with respect to the L^2 -inner product $\langle \mathbf{u}, \mathbf{v} \rangle = \int_0^L \mathbf{u} \cdot \bar{\mathbf{v}} dx$:

$$\mathcal{L}_1^H \psi = \mathbf{0}, \quad \text{with} \quad \mathcal{L}_1^H = -\frac{d}{dx} + \begin{pmatrix} -i\bar{\lambda}_0 & -i\bar{r}_0 \\ i\bar{q}_0 & i\bar{\lambda}_0 \end{pmatrix}.$$

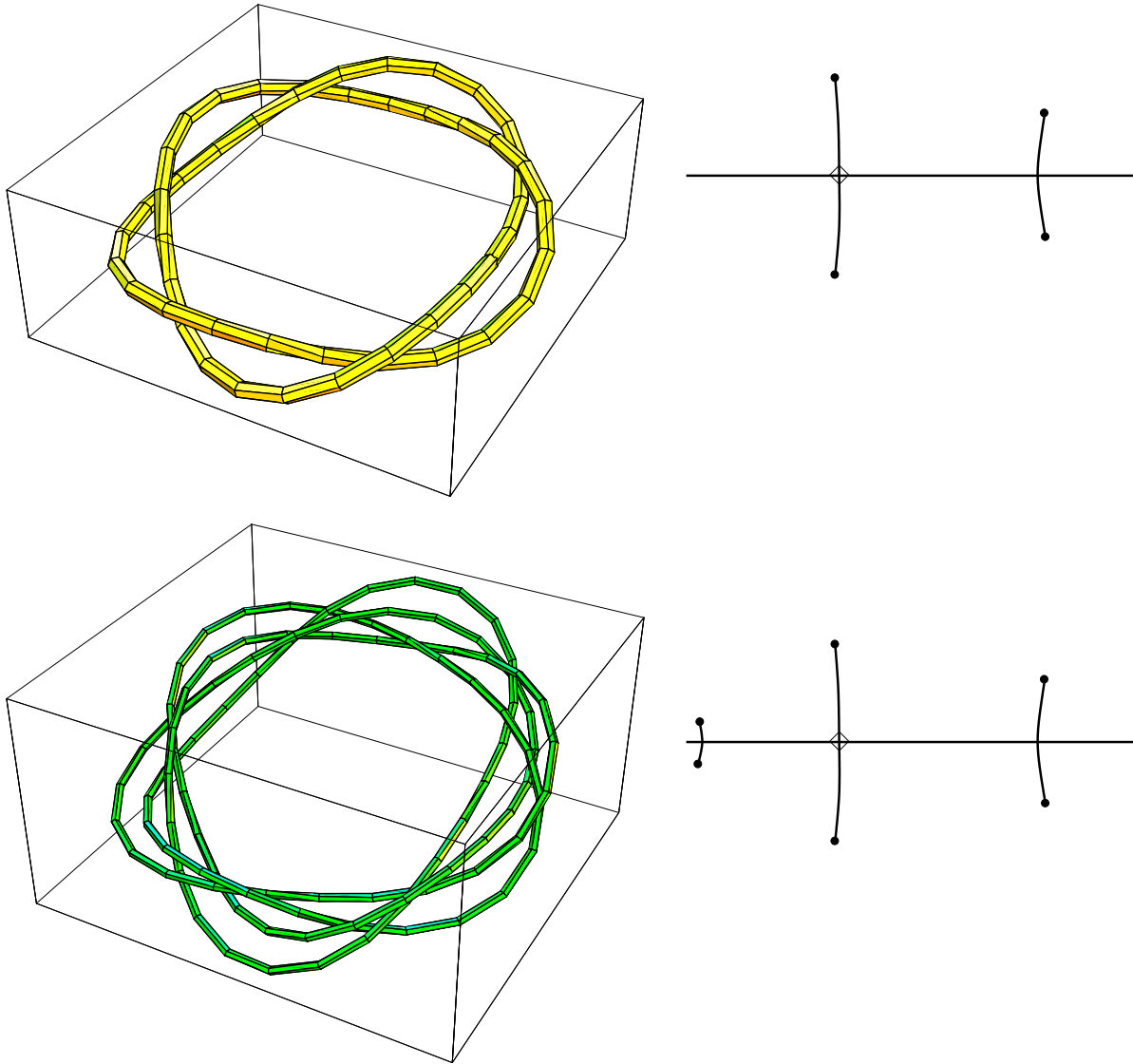


FIGURE 2. Results of the two-step deformation $[4; -10, 7]$. The end of the first step is the left-hand $(2, -5)$ torus knot shown at top, and the result of the second step is the knot shown at bottom, which is a right-hand $(2, 7)$ cable on the torus knot. Approximate diagrams of the Floquet spectrum appear at right; in these, the reconstruction point is marked by a diamond, while double points are not shown.

(The “formal adjoint” is computed neglecting boundary conditions. It turns out that the solvability condition of system (15) is correctly expressed in terms of the formal adjoint, as discussed below.) Taking the inner product of both sides of (15) with a solution of $\mathcal{L}_1^H \psi = \mathbf{0}$ leads to the *solvability condition* for system (15), requiring that its right-hand side is orthogonal to any solution of the homogeneous formal adjoint system.

Since λ_0 is assumed to be a real double point, it is removable [28]. This means that the space of solutions of $\mathcal{L}_1 \phi = \mathbf{0}$ is spanned by the two linearly independent Bloch eigenfunctions

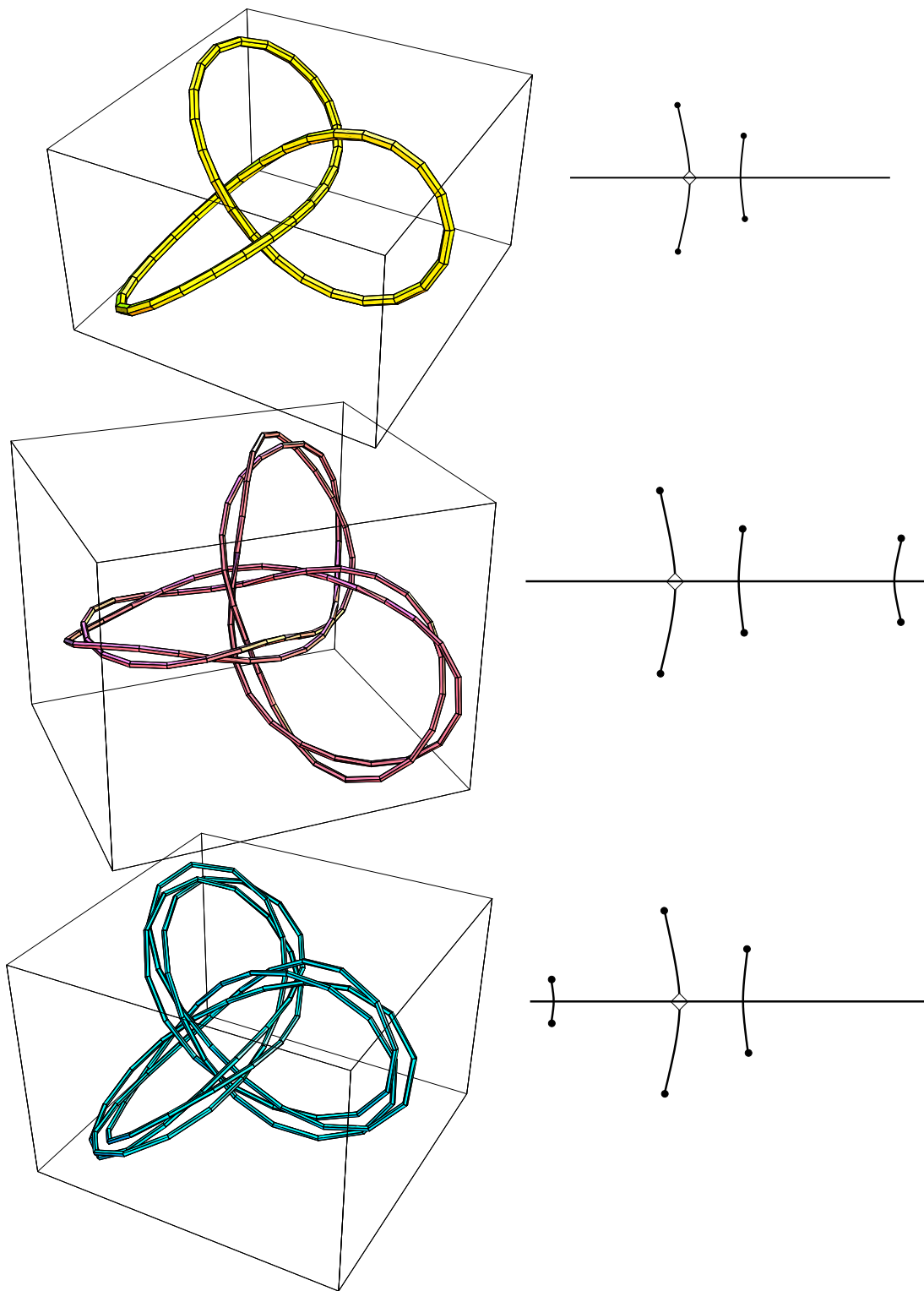


FIGURE 3. Results of the two-step deformations $[4; -6, -13]$ (in the middle) and $[6; -9, 10]$ (at bottom). In both cases, the result of the first step of the deformation gives the left-hand trefoil shown at top. The $[4; -6, -13]$ is a left-hand $(2, -13)$ cable on the trefoil, while the $[6; -9, 10]$ is a right-hand $(3, 5)$ cable on the trefoil.

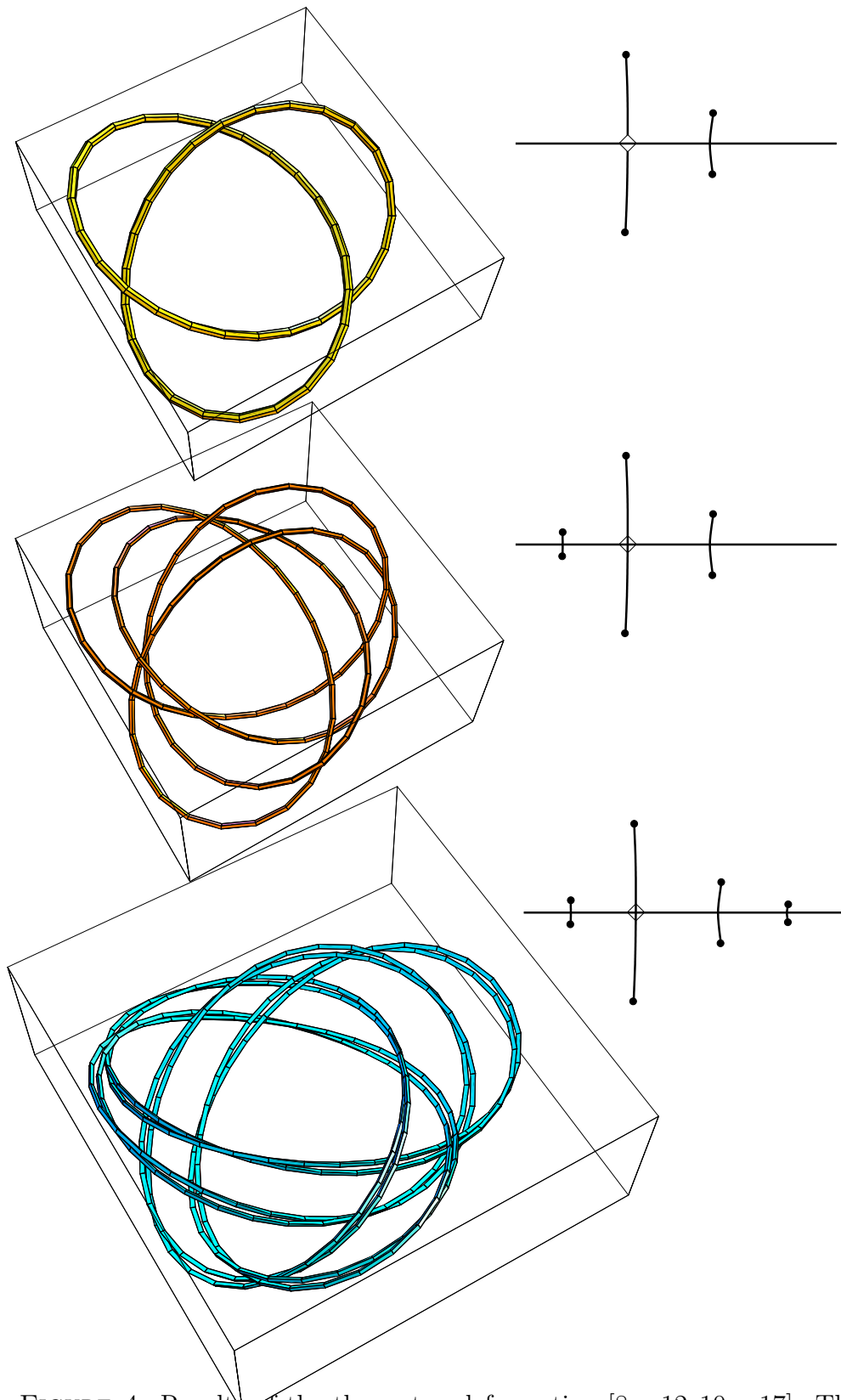


FIGURE 4. Results of the three-step deformation $[8; -12, 10, -17]$. The first step gives the left-hand trefoil shown at top, the second step (shown in the middle) gives a right-hand $(2, 5)$ cable on the trefoil, and the third step (shown at bottom) gives a left-hand $(2, -17)$ cable on the previous cable.

(see §6)

$$\boldsymbol{\varphi}^+ = \begin{pmatrix} \varphi_1^+ \\ \varphi_2^+ \end{pmatrix}, \quad \boldsymbol{\varphi}^- = \begin{pmatrix} \varphi_1^- \\ \varphi_2^- \end{pmatrix},$$

evaluated at λ_0 . It is easy to show that a basis for the solution space of the adjoint system $\mathcal{L}_1^H \boldsymbol{\psi} = \mathbf{0}$ is given by

$$J\overline{\boldsymbol{\varphi}}^+ = \begin{pmatrix} \overline{\varphi_2^+} \\ -\overline{\varphi_1^+} \end{pmatrix}, \quad J\overline{\boldsymbol{\varphi}}^- = \begin{pmatrix} \overline{\varphi_2^-} \\ -\overline{\varphi_1^-} \end{pmatrix},$$

where J is the symplectic matrix $\begin{pmatrix} 0 & -1 \\ 1 & 0 \end{pmatrix}$. Substituting $\boldsymbol{\phi}_0 = a\boldsymbol{\varphi}^+ + b\boldsymbol{\varphi}^-$, a general solution of $\mathcal{L}_1 \boldsymbol{\phi} = \mathbf{0}$, in system (15), we compute the solvability condition to be the following system in the unknowns a and b :

$$\begin{aligned} & \left[2i\lambda_1 \int_0^L \varphi_1^+ \varphi_2^+ dx + i \left\langle \mathbf{q}_1, J \begin{pmatrix} \overline{(\varphi_1^+)^2} \\ -(\varphi_2^+)^2 \end{pmatrix} \right\rangle \right] a + \left[i\lambda_1 \int_0^L (\varphi_1^+ \varphi_2^- + \varphi_2^+ \varphi_1^-) dx + i \left\langle \mathbf{q}_1, J \begin{pmatrix} \overline{\varphi_1^+ \varphi_1^-} \\ -\varphi_2^+ \varphi_2^- \end{pmatrix} \right\rangle \right] b = 0, \\ & \left[i\lambda_1 \int_0^L (\varphi_1^+ \varphi_2^- + \varphi_2^+ \varphi_1^-) dx + i \left\langle \mathbf{q}_1, J \begin{pmatrix} \overline{\varphi_1^+ \varphi_1^-} \\ -\varphi_2^+ \varphi_2^- \end{pmatrix} \right\rangle \right] a + \left[2i\lambda_1 \int_0^L \varphi_1^- \varphi_2^- dx + i \left\langle \mathbf{q}_1, J \begin{pmatrix} \overline{(\varphi_1^-)^2} \\ -(\varphi_2^-)^2 \end{pmatrix} \right\rangle \right] b = 0, \end{aligned}$$

where the various components of the Bloch eigenfunctions are evaluated at the double points λ_0 .

For a removable double point λ_d , the following identities hold

$$\int_0^L \varphi_1^+ \varphi_2^+ |_{\lambda_d} dx = 0, \quad \int_0^L \varphi_1^- \varphi_2^- |_{\lambda_d} dx = 0,$$

as shown, for example, in [15]. Thus, the condition for existence of a nontrivial solution (a, b) of the above system (amounting to the vanishing of the determinant of the associated matrix) provides the selection of the perturbation of the affected double point. A simple calculation gives

$$\lambda_1 = \frac{\left\langle \mathbf{q}_1, J \begin{pmatrix} \overline{\varphi_1^+ \varphi_1^-} \\ -\varphi_2^+ \varphi_2^- \end{pmatrix} \right\rangle |_{\lambda_0} \pm \sqrt{\left\langle \mathbf{q}_1, J \begin{pmatrix} \overline{(\varphi_1^+)^2} \\ -(\varphi_2^+)^2 \end{pmatrix} \right\rangle |_{\lambda_0} \left\langle \mathbf{q}_1, J \begin{pmatrix} \overline{(\varphi_1^-)^2} \\ -(\varphi_2^-)^2 \end{pmatrix} \right\rangle |_{\lambda_0}}}{\int_0^L (\varphi_1^+ \varphi_2^- + \varphi_2^+ \varphi_1^-) |_{\lambda_0} dx},$$

where \mathbf{q}_1 denotes the vector $(q_1, r_1)^T$.

We now recall that certain vectors of quadratic products of components of the Bloch eigenfunctions (the *squared eigenfunctions*) form a basis for $L_{per}^2([0, L], \mathbb{C})$. (See §6 and references therein.) Moreover, we can write a generic periodic perturbation \mathbf{q}_1 as a linear combination of the elements of the basis of *squared eigenfunctions*:

$$\begin{aligned} \begin{pmatrix} q_1 \\ r_1 \end{pmatrix} = & \sum_{\text{simple points } \lambda_s} c_s \begin{pmatrix} \phi_1^2 \\ -\phi_2^2 \end{pmatrix} |_{\lambda_s} + \sum_{\text{critical non-per. pts } \lambda_c} d_s \begin{pmatrix} \varphi_1^+ \varphi_1^- \\ -\varphi_2^+ \varphi_2^- \end{pmatrix} |_{\lambda_c} \\ & + \sum_{\text{remov. double pts } \lambda_d} [e_d^+ \begin{pmatrix} (\varphi_1^+)^2 \\ -(\varphi_2^+)^2 \end{pmatrix} + e_d^- \begin{pmatrix} (\varphi_1^-)^2 \\ -(\varphi_2^-)^2 \end{pmatrix}] |_{\lambda_d}. \end{aligned}$$

(We have assumed for simplicity that the potential \mathbf{q}_0 possesses no non-removable double points and no periodic points of multiplicity higher than two.)

Because of the biorthogonality property of the squared eigenfunctions (see §6), we compute

$$\left\langle \mathbf{q}_1, J \begin{pmatrix} \overline{\varphi_1^+ \varphi_1^-} \\ -\varphi_2^+ \varphi_2^- \end{pmatrix} \Big|_{\lambda_0} \right\rangle = 0,$$

$$\left\langle \mathbf{q}_1, J \begin{pmatrix} (\overline{\varphi_1^+})^2 \\ -(\overline{\varphi_2^+})^2 \end{pmatrix} \Big|_{\lambda_0} \right\rangle = e_0^- \left\langle \begin{pmatrix} (\varphi_1^-)^2 \\ -(\varphi_2^-)^2 \end{pmatrix}, J \begin{pmatrix} (\overline{\varphi_1^+})^2 \\ -(\overline{\varphi_2^+})^2 \end{pmatrix} \right\rangle \Big|_{\lambda_0} = -e_0^- \left\langle \begin{pmatrix} (\varphi_1^+)^2 \\ -(\varphi_2^+)^2 \end{pmatrix}, J \begin{pmatrix} (\overline{\varphi_1^-})^2 \\ -(\overline{\varphi_2^-})^2 \end{pmatrix} \right\rangle \Big|_{\lambda_0}$$

and

$$\left\langle \mathbf{q}_1, J \begin{pmatrix} (\overline{\varphi_1^-})^2 \\ -(\overline{\varphi_2^-})^2 \end{pmatrix} \Big|_{\lambda_0} \right\rangle = e_0^+ \left\langle \begin{pmatrix} (\varphi_1^+)^2 \\ -(\varphi_2^+)^2 \end{pmatrix}, J \begin{pmatrix} (\overline{\varphi_1^-})^2 \\ -(\overline{\varphi_2^-})^2 \end{pmatrix} \right\rangle \Big|_{\lambda_0},$$

with normalization coefficient (see Lemma 6.3)

$$\left\langle \begin{pmatrix} (\varphi_1^+)^2 \\ -(\varphi_2^+)^2 \end{pmatrix}, J \begin{pmatrix} (\overline{\varphi_1^-})^2 \\ -(\overline{\varphi_2^-})^2 \end{pmatrix} \right\rangle \Big|_{\lambda_0} = \frac{1}{2i} \sqrt{\Delta(\lambda_0) \Delta''(\lambda_0)} |W[\varphi^+, \varphi^-]|_{\lambda_0}^2,$$

where $W[\varphi^+, \varphi^-]$ denotes the Wronskian of the two Bloch eigenfunctions. Because the normalization coefficient is non zero, it follows that the real double point λ_0 will split at first order and none of the remaining double point will if and only if the perturbation \mathbf{q}_1 contains only terms of the form

$$e_0^+ \begin{pmatrix} (\varphi_1^+)^2 \\ -(\varphi_2^+)^2 \end{pmatrix} \Big|_{\lambda_0} + e_0^- \begin{pmatrix} (\varphi_1^-)^2 \\ -(\varphi_2^-)^2 \end{pmatrix} \Big|_{\lambda_0}.$$

and none of the terms $e_d^+ \begin{pmatrix} (\varphi_1^+)^2 \\ -(\varphi_2^+)^2 \end{pmatrix} \Big|_{\lambda_d} + e_d^- \begin{pmatrix} (\varphi_1^-)^2 \\ -(\varphi_2^-)^2 \end{pmatrix} \Big|_{\lambda_d}$.

Analogous results can be deduced by computing expressions for the first order variation of simple and critical points: they will move at first order if and only if the potential \mathbf{q}_1 contains terms of the form $\begin{pmatrix} \varphi_1^2 \\ -\varphi_2^2 \end{pmatrix} \Big|_{\lambda_s}$ or $\begin{pmatrix} \varphi_1^+ \varphi_1^- \\ -\varphi_2^+ \varphi_2^- \end{pmatrix} \Big|_{\lambda_c}$ respectively. Thus, because we are assuming that these points do not move to first order, then these terms do not occur in \mathbf{q}_1 .

Since λ_0 is assumed to be real, the Bloch eigenfunctions possess the additional symmetry $\varphi^- = \overline{J\varphi^+}$, thus a perturbation \mathbf{q}_1 that splits only λ_0 , leaving the rest of the discrete spectrum and critical points invariant at first order must be of the form:

$$\begin{pmatrix} q_1 \\ r_1 \end{pmatrix} = \begin{pmatrix} e_0^+ (\varphi_1^+)^2 + e_0^- (\varphi_2^+)^2 \\ -[e_0^+ (\varphi_2^+)^2 + e_0^- (\varphi_1^+)^2] \end{pmatrix} \Big|_{\lambda_0}.$$

Finally, requiring that the focussing reality constraints $r_1 = -\overline{q_1}$ be satisfied leads to the condition

$$(e_0^+ - \overline{e_0^-}) (\varphi_2^+)^2 - (\overline{e_0^+} - e_0^-) (\varphi_1^+)^2 = 0,$$

and, given the linear independence of $(\varphi_1^+)^2$ and $(\varphi_2^+)^2$ over \mathbb{C} , one obtains $e_0^+ = \overline{e_0^-} = c$ for some complex constant c . We summarize these results in the following

Proposition 4.1. *Suppose the periodic potential q_0 undergoes a smooth perturbation $q = q_0 + \varepsilon q_1$ and its spectrum deforms isoperiodically in such a way a unique real double point λ_0 splits at first order, while all other points the discrete spectrum as well as the critical points remain unchanged up to first order. If, in addition, the deformation preserves the reality of the potential, then the perturbation must have the form $q_1 = \operatorname{Re}(c)[(\varphi_1^+)^2 + (\overline{\varphi_2^+})^2] \Big|_{\lambda_0} +$*

$i \operatorname{Im}(c)[(\varphi_1^+)^2 - (\overline{\varphi_2^+})^2] \Big|_{\lambda_0}$, with $c \in \mathbb{C}$. Moreover, the affected double point splits at first order in the following pair of simple points

$$\lambda_{\pm} = \lambda_0 \pm i\epsilon|c|^2 \frac{|W[\varphi^+, \varphi^-]|^2 \sqrt{|\Delta''(\lambda_0)|}}{\int_0^L (|\varphi_1^+|^2 - |\varphi_2^+|^2) dx} + O(\epsilon^2).$$

5. THE CABLING THEOREM

In this section we will assume that q_0 is an NLS potential of period $n\pi$, obtained by a sequence of g homotopic deformations from that of the n -times covered circle, notated as $[n; m_1, \dots, m_g]$, and that λ_0 is a double point of the $jn\pi$ -periodic spectrum of q_0 whose original position (in the spectrum of the circle, before the deformations) was $-\sqrt{(m/(jn))^2 - 1}$ times the sign of m , where m is an integer whose magnitude is greater than j and which is relatively prime to j . We will show that, if we perturb q_0 as in Proposition 4.1, then the perturbed curve $\gamma = \gamma_0 + \epsilon\gamma_1 + O(\epsilon^2)$ is an (j, m) -cable on γ_0 for sufficiently small ϵ .

We also need to assume that q_0 is sufficiently close to the plane wave potential; we will be more specific about this assumption at the end of this section.

5.1. Perturbed Potentials and Perturbed Curves via the Sym Formula. We will begin by calculating the perturbation of the curve. We assume that

$$q(x, t; \epsilon) = q_0 + \epsilon q_1 + O(\epsilon^2)$$

is a one-parameter family of NLS solutions, and

$$\Phi(x, t; \lambda, \epsilon) = \Phi_0 + \epsilon\Phi_1 + O(\epsilon^2),$$

is a fundamental matrix solution for the AKNS system at (q, λ) . To be specific, we will assume that $\Phi(0, 0; \lambda, \epsilon)$ is the identity matrix. Moreover, when λ is real, we can assume that Φ takes the form $[\phi, J\overline{\phi}]$. We will also assume that q_1 is expressed as a linear combination of squared eigenfunctions for the AKNS system at (q_0, λ_0) , where λ_0 is a double point for q_0 . (This assumption was justified, for isoperiodic deformations that open up a double point, in the previous section.)

For use in the Sym-Pohlmeyer formula (6), we will need to calculate Φ_1 at $\lambda = \Lambda_0$, the reconstruction point. (Although this reconstruction point will vary under isoperiodic deformation, Proposition 2.1 ensures that it is fixed up to $O(\epsilon^2)$.) For the sake of brevity, we will use the abbreviations

$$\varphi_1 = \varphi_1^+(q_0, \lambda_0), \quad \varphi_2 = \varphi_2^+(q_0, \lambda_0),$$

where φ^+ is one of the Bloch eigenfunctions, as normalized in (32). Then the results of §4 imply that

$$q_1 = c(\varphi_1)^2 + \overline{c}(\overline{\varphi_2})^2 \tag{16}$$

for some complex constant c . We will also let

$$\Phi_0(x, t; \lambda) = \begin{pmatrix} \phi_1 & -\overline{\phi_2} \\ \phi_2 & \overline{\phi_1} \end{pmatrix}, \tag{17}$$

where we will leave λ arbitrary (but real) for the moment, but later set $\lambda = \Lambda_0$.

Setting $B_1 = \Phi_1(\Phi_0)^{-1}$ and taking the ϵ term on each side of the AKNS system gives

$$\frac{d}{dx} B_1 = \Phi_0^{-1} Q_1 \Phi_0, \quad Q_1 = \begin{pmatrix} 0 & iq_1 \\ i\overline{q_1} & 0 \end{pmatrix}$$

(see [5] for more details). Expanding the inverse, we get

$$\frac{d}{dx} B_1 = \frac{i}{D} \begin{pmatrix} q_1 \bar{\phi}_1 \phi_2 + \bar{q}_1 \phi_1 \bar{\phi}_2 & q_1 \bar{\phi}_1^2 - \bar{q}_1 \bar{\phi}_2^2 \\ \bar{q}_1 \phi_1^2 - q_1 \phi_2^2 & -q_1 \bar{\phi}_1 \phi_2 - \bar{q}_1 \phi_1 \bar{\phi}_2 \end{pmatrix}, \quad (18)$$

where $D = \det \Phi_0 = |\phi_1|^2 + |\phi_2|^2$, which is independent of x and t .

To compute B_1 , we need to take antiderivatives of the entries of the matrix appearing on the right-hand side of (18). (Because the matrix takes value in $\mathfrak{su}(2)$, it suffices to find antiderivatives for entries in the first column.) To do this we will use special properties of solutions of the squared eigenfunction system (28),(29) Recall that if $\phi, \tilde{\phi}$ are two vector solutions of the AKNS system at the same λ -value, then the construction

$$\begin{bmatrix} f \\ g \\ h \end{bmatrix} = \phi \otimes \tilde{\phi} = \begin{bmatrix} \frac{1}{2}(\phi_1 \tilde{\phi}_2 + \tilde{\phi}_1 \phi_2) \\ \phi_1 \tilde{\phi}_1 \\ -\phi_2 \tilde{\phi}_2 \end{bmatrix} \quad (19)$$

gives a solution of the squared eigenfunction system (28),(29) (see §6.1 in the Appendix). Furthermore, if (f, g, h) and $(\hat{f}, \hat{g}, \hat{h})$ are solutions of this system at (q_0, λ) and $(q_0, \hat{\lambda})$ respectively, then

$$\frac{d}{dx} (g\hat{h} + \hat{g}h - 2f\hat{f}) = 2i(\lambda - \hat{\lambda})(\hat{g}h - g\hat{h}). \quad (20)$$

(This can be easily verified from the system of ODE's (28) satisfied by (f, g, h) ; see, for example, the proof of Theorem 2.1 in [24].)

To get the top left entry in (18), let $\hat{g} = q_1$, $\hat{h} = -\bar{q}_1$, $\hat{\lambda} = \lambda_0$, and $g = \phi_1 \bar{\phi}_2$, $h = \phi_2 \bar{\phi}_1$ (the latter arising from the construction $\phi \otimes (J\bar{\phi})$, giving $f = -\frac{1}{2}(|\phi_1|^2 - |\phi_2|^2)$). Then

$$\int q_1 \bar{\phi}_1 \phi_2 + \bar{q}_1 \phi_1 \bar{\phi}_2 \, dx = \frac{1}{2i(\lambda - \lambda_0)} \left(q_1 \bar{\phi}_1 \phi_2 - \bar{q}_1 \phi_1 \bar{\phi}_2 - (|\phi_1|^2 - |\phi_2|^2) \hat{f} \right),$$

where, using the formula (16) for q_1 , we have

$$\hat{f} = c\varphi_1\varphi_2 - \bar{c}\bar{\varphi}_1\bar{\varphi}_2.$$

To get the bottom left entry in (18) (up to a factor of minus one), we keep $\hat{f}, \hat{g}, \hat{h}$ the same, and change to $g = \phi_1^2$ and $h = -\phi_2^2$ (arising from the construction $\phi \otimes \phi$, giving $f = \phi_1 \phi_2$). Then

$$\int q_1 \phi_2^2 - \bar{q}_1 \phi_1^2 \, dx = \frac{1}{2i(\lambda - \lambda_0)} \left(\bar{q}_1 \phi_1^2 + q_1 \phi_2^2 - 2\phi_1 \phi_2 \hat{f} \right).$$

So, up to an additive constant, we obtain

$$B_1 = \frac{1}{2(\lambda - \lambda_0)D} \begin{pmatrix} -\bar{q}_1 \phi_1 \bar{\phi}_2 + q_1 \bar{\phi}_1 \phi_2 - (|\phi_1|^2 - |\phi_2|^2) \hat{f} & q_1 \bar{\phi}_1^2 + \bar{q}_1 \bar{\phi}_2^2 + 2\bar{\phi}_1 \bar{\phi}_2 \hat{f} \\ -\bar{q}_1 \phi_1^2 - q_1 \phi_2^2 + 2\phi_1 \phi_2 \hat{f} & \bar{q}_1 \phi_1 \bar{\phi}_2 - q_1 \bar{\phi}_1 \phi_2 + (|\phi_1|^2 - |\phi_2|^2) \hat{f} \end{pmatrix}.$$

Substituting $\Phi = \Phi_0(I + \epsilon B_1 + O(\epsilon^2))$ into the Sym-Pohlmeyer formula gives

$$\gamma = \gamma_0 + \epsilon \gamma_1 + O(\epsilon^2), \quad \gamma_0 = \Phi_0^{-1} \frac{d\Phi_0}{d\lambda}, \quad \gamma_1 = \frac{dB_1}{d\lambda} + [\gamma_0, B_1].$$

(Recall that we are identifying matrices in $\mathfrak{su}(2)$ with vectors in \mathbb{R}^3 .) But $B_1 = \int \Phi_0^{-1} Q_1 \Phi_0 dx$, and Q_1 is independent of λ , so

$$\begin{aligned} \frac{dB_1}{d\lambda} &= \int -\gamma_0 \Phi_0^{-1} Q_1 \Phi_0 + \Phi_0^{-1} Q_1 \frac{d\Phi_0}{d\lambda} dx = \int [\Phi_0^{-1} Q_1 \Phi_0, \gamma_0] dx \\ &= \int [(B_1)_x, \gamma_0] dx = [B_1, \gamma_0] - \int [B_1, T] dx, \end{aligned}$$

where integration by parts is used in the second line. Therefore, $\gamma_1 = \int [T, B_1] dx$, where

$$T = \Phi_0^{-1} \begin{pmatrix} -i & 0 \\ i & 0 \end{pmatrix} \Phi_0 = \frac{1}{D} \begin{pmatrix} -i(|\phi_1|^2 - |\phi_2|^2) & 2i\bar{\phi}_1\bar{\phi}_2 \\ 2i\phi_1\phi_2 & i(|\phi_1|^2 - |\phi_2|^2) \end{pmatrix}.$$

We now set $\lambda = \Lambda_0$, the reconstruction point that generates the closed curve γ_0 from potential q_0 . Thus, because $\int T dx = 0$, the additive constant in B_1 does not change the value of γ_1 .

Note that the coefficient of \hat{f} in B_1 is an exact multiple of the matrix T . So,

$$\begin{aligned} [T, B_1] &= \frac{i}{2D^2(\Lambda_0 - \lambda_0)} \left[\begin{pmatrix} |\phi_2|^2 - |\phi_1|^2 & 2\bar{\phi}_1\bar{\phi}_2 \\ 2\phi_1\phi_2 & |\phi_1|^2 - |\phi_2|^2 \end{pmatrix}, \begin{pmatrix} -\bar{q}_1\phi_1\bar{\phi}_2 + q_1\bar{\phi}_1\phi_2 & q_1\bar{\phi}_1^2 + \bar{q}_1\bar{\phi}_2^2 \\ -\bar{q}_1\phi_1^2 - q_1\phi_2^2 & \bar{q}_1\phi_1\bar{\phi}_2 - q_1\bar{\phi}_1\phi_2 \end{pmatrix} \right] \\ &= \frac{i}{D(\Lambda_0 - \lambda_0)} \begin{pmatrix} -q_1\bar{\phi}_1\phi_2 - \bar{q}_1\phi_1\bar{\phi}_2 & -q_1\bar{\phi}_1^2 + \bar{q}_1\bar{\phi}_2^2 \\ \bar{q}_1\phi_1^2 - q_1\phi_2^2 & -q_1\phi_1\phi_2 - \bar{q}_1\phi_1\bar{\phi}_2 \end{pmatrix}. \end{aligned}$$

Amazingly, the quantities we have to integrate are the same as before; in fact,

$$[T, B_1] = \frac{-1}{(\Lambda_0 - \lambda_0)} \frac{dB_1}{dx}.$$

Therefore,

$$\begin{aligned} \gamma_1 &= \frac{-1}{\Lambda_0 - \lambda_0} B_1 \\ &= \frac{-1}{2(\Lambda_0 - \lambda_0)^2 D} \left(q_1 \begin{pmatrix} \bar{\phi}_1\phi_2 & \phi_1^2 \\ -\phi_2^2 & -\bar{\phi}_1\phi_2 \end{pmatrix} + \bar{q}_1 \begin{pmatrix} -\phi_1\bar{\phi}_2 & \bar{\phi}_2^2 \\ -\phi_1^2 & \phi_1\bar{\phi}_2 \end{pmatrix} + \hat{f} \begin{pmatrix} |\phi_2|^2 - |\phi_1|^2 & 2\bar{\phi}_1\bar{\phi}_2 \\ 2\phi_1\phi_2 & |\phi_1|^2 - |\phi_2|^2 \end{pmatrix} \right) \end{aligned}$$

When we expand this in terms of the Λ_0 -natural frame of γ_0 , comprising T with

$$U_1 = \Phi_0^{-1} \begin{pmatrix} 0 & 1 \\ -1 & 0 \end{pmatrix} \Phi_0, \quad U_2 = \Phi_0^{-1} \begin{pmatrix} 0 & i \\ i & 0 \end{pmatrix} \Phi_0,$$

then we obtain the first order perturbation term in the expression for the curve

$$\gamma_1 = \frac{-1}{2(\Lambda_0 - \lambda_0)^2} \left(-i\hat{f}T + \operatorname{Re}(q_1)U_1 + \operatorname{Im}(q_1)U_2 \right). \quad (21)$$

5.2. Natural Frames Unlinked. Now that we have a nice expression for the components of the perturbed curve in terms of a natural frame, we will show that under some circumstances the perturbed curve $\gamma_0 + \epsilon\gamma_1$ forms a cable around the unperturbed curve γ_0 . To determine the type of the cable correctly, we need to know if the natural frame itself winds around γ_0 . We will show that, for sufficiently small ϵ , the curve $\gamma_0 + \epsilon U_1$ is unlinked with γ_0 —provided that γ_0 has self-linking number zero and has no inflection points. Note that, because the self-linking number is a discrete invariant—either an integer or a half-integer—it does not change under deformation, and is multiplied by the integer n when we pass from a curve to its n -fold cover. Therefore, any curve that is obtained from the circle by a succession of multiple-coverings and deformations will also have zero self-linking number.

According to White's formula [31], the linking number of γ_0 and $\gamma_0 + \epsilon U_1$

$$\text{Lk}(\gamma_0, \gamma_0 + \epsilon U_1) = \text{Wr}(\gamma_0) + \frac{1}{2\pi} \int (T \times U_1) dU_1.$$

Because $dU_1/dx = -k_1 T + \Lambda_0 U_2$ (where x is arclength) and $U_2 = T \times U_1$, then

$$\text{Lk}(\gamma_0, \gamma_0 + \epsilon U_1) = \text{Wr}(\gamma_0) + \frac{L\Lambda_0}{2\pi},$$

where L is the length of γ_0 . Meanwhile, the writhe $\text{Wr}(\gamma_0)$ is related to the self-linking number by Pohl's formula [25]

$$\text{SL}(\gamma_0) = \text{Wr}(\gamma_0) + \frac{1}{2\pi} \int \tau dx.$$

Taking $\text{SL}(\gamma_0)$ to be zero, we get

$$\text{Lk}(\gamma_0, \gamma_0 + \epsilon U_1) = \frac{1}{2\pi} \int (\Lambda_0 - \tau) dx.$$

We can relate the last integrand to the unperturbed potential $q_0 = \frac{1}{2}(k_1 + ik_2)$ written in terms of the natural curvatures, by making use of the Frenet equations and the natural frame equations. Differentiating each side of the expression

$$\kappa N = k_1 U_1 + k_2 U_2$$

for the Frenet normal in terms of the natural frame vectors, and cancelling out tangent terms on both sides gives

$$\kappa_x N + \kappa \tau B = (k_1)_x U_1 + (k_2)_x U_2 + k_1 \Lambda_0 U_2 - k_2 \Lambda_0 U_1.$$

Next, dotting both sides of the with $\kappa B = T \times \kappa N = k_1 U_2 - k_2 U_1$ gives

$$\kappa^2 \tau = k_1 (k_2)_x - k_2 (k_1)_x + \Lambda_0 \kappa^2.$$

So,

$$\Lambda_0 - \tau = - \left(\frac{k_1 (k_2)_x - k_2 (k_1)_x}{\kappa^2} \right) = - \text{Im}((q_0)_x / q_0).$$

Now, the value Λ_0 is chosen so that q_0 is periodic along the curve. So, provided that q_0 is nonvanishing along the curve (and, this is true if γ_0 is sufficiently close to a multiply-covered circle) then the integral is zero, and the natural frame is unlinked.

Thus, the knotting of the perturbed curve about γ_0 is completely determined by the behavior of q_1 .

5.3. Monotonicity of Argument. In Section 4 we showed that if q_1 only contains terms associated to the double point being opened up at first order, then it must be of the form (16). We will establish that the argument of this function is monotone in x by calculating it for the multiply-covered circle, and invoking continuous dependence on the potential.

As an exercise, one can calculate the following Baker eigenfunction for the plane wave solution $q = \exp(2it)$ for real values of λ :

$$\psi(x, t; \lambda) = \frac{\exp(ikx + 2ik\lambda t)}{k + \lambda + 1} \begin{bmatrix} \exp(it) \\ (k + \lambda) \exp(-it) \end{bmatrix},$$

where $k = \sqrt{\lambda^2 + 1}$. This expression extends to the spectral curve $\mu^2 = \lambda^2 + 1$ associated to the plane wave solution by replacing k with μ , and coincides with the expression of the Baker-Akhiezer eigenfunction normalized as in [6].

We then calculate that

$$c\psi_1^2 + \bar{c}\bar{\psi}_2^2 = \exp(2it) \frac{u + \bar{u}(k + \lambda)^2}{(k + \lambda + 1)^2}$$

where $u := c \exp(2ikx + 4ik\lambda t)$. (Note that λ and k are assumed to be real.) Because $du/dx = 2iku$, then

$$\frac{d}{dx} \log \left(c\psi_1^2 + \bar{c}\bar{\psi}_2^2 \right) = 2ik \frac{u - (k + \lambda)^2 \bar{u}}{u + (k + \lambda)^2 \bar{u}}.$$

Then

$$\begin{aligned} \operatorname{Im} \frac{d}{dx} \log \left(c\psi_1^2 + \bar{c}\bar{\psi}_2^2 \right) &= 2k \operatorname{Re} \frac{u - (k + \lambda)^2 \bar{u}}{u + (k + \lambda)^2 \bar{u}} = 2k \operatorname{Re} \frac{(1 + (k + \lambda)^4) |u|^2 + (k + \lambda)^2 (u^2 - \bar{u}^2)}{|u + (k + \lambda)^2 \bar{u}|^2} \\ &= 2k |u|^2 \frac{(1 - (k + \lambda)^2)(1 + (k + \lambda)^2)}{|u + (k + \lambda)^2 \bar{u}|^2} = -4k\lambda |c|^2 \frac{(k + \lambda)(1 + (k + \lambda)^2)}{|u + (k + \lambda)^2 \bar{u}|^2}, \end{aligned} \quad (22)$$

where in the last step we use the fact that $k^2 = 1 + \lambda^2$ to write $1 - (k + \lambda)^2 = -2\lambda(k + \lambda)$.

The sign of this quantity explains why opening up double points where $\lambda > 0$ leads to left-handed cables, and $\lambda < 0$ leads to right-handed cables. In the next section, we will determine the type of this cable.

5.4. Cable Type. Given a knot $K_1 : S^1 \rightarrow \mathbb{R}^3$ whose image lies inside a solid torus T^3 , and a knot $K_2 : S^2 \rightarrow \mathbb{R}^3$, we can form a satellite knot on $K_3 = \tau \circ K_1$, where τ is a diffeomorphism from T^3 to a tubular neighborhood of the image of K_2 . In particular, when K_1 is a (p, q) torus knot, then K_3 is a (p, q) cable on K_2 .

Because the natural frames of γ_0 are unlinked, we can use them to define a diffeomorphism δ from $S^1 \times D^2$ to a tubular neighborhood of γ_0 , given by

$$\delta : (z, r, \theta) \mapsto \gamma_0(z) + (r \cos \theta) U_1(z) + (r \sin \theta) U_2(z),$$

where z, r, θ are cylindrical coordinates, with r less than one half of the minimum radius of curvature of γ_0 , and we think of $S^1 \times D^2$ as the quotient of the solid cylinder by the equivalence relation $z \sim z + L$.

By (21), the perturbed curve is

$$\gamma(x) = \gamma_0(x) - \frac{\epsilon}{2(\Lambda_0 - \lambda_0)^2} \left(-i\hat{f}T + \operatorname{Re}(q_1) U_1 + \operatorname{Im}(q_1) U_2 \right) + O(\epsilon^2).$$

Consider the modification

$$\tilde{\gamma}(x) = \gamma_0(x) - \frac{\epsilon}{2(\Lambda_0 - \lambda_0)^2} (\operatorname{Re}(q_1) U_1 + \operatorname{Im}(q_1) U_2),$$

which, by continuity, will have the same knot type as $\gamma(x)$ for ϵ sufficiently small. Because q_1 is composed of quadratic products of eigenfunctions, which have the form (10), the period of q_1 is the lowest common multiple of $L = n\pi$ and $\pi/\Omega_1(\lambda_0)$. Because the isoperiodic deformations preserve the value of $\Omega_1(\lambda_0)$, we can compute it by running the deformations backwards to the multiply-covered circle. Specifically, suppose that $[n; m_1, \dots, m_g]$ is the deformation scheme that produced q_0 . Then, upon running the deformation steps backwards, the basepoint for Ω_1 limits to $-i$. So,

$$\Omega_1(\lambda_0) = \int_{-i}^{\sqrt{(m/(jn))^2 - 1}} \frac{\lambda}{\sqrt{\lambda^2 + 1}} d\lambda = \frac{|m|}{jn}.$$

Hence, $\pi/\Omega_1(\lambda_0) = jL/|m|$, and the period of q_1 is jL . (Recall that j and m are coprime.)

The image of $\tilde{\gamma}(x)$ under the inverse of δ is the curve

$$z = x, \quad r = \epsilon |q_1(x)| / (2(\Lambda_0 - \lambda_0)^2), \quad \theta = \arg(-q_1(x)).$$

Note that r is never zero along this curve, so that it never crosses the z -axis. Consider the map $\bar{\theta} : S^1 \rightarrow S^1$ defined by $x \mapsto \arg(q_1(x))$, where the domain S^1 is \mathbb{R} modulo jL and the codomain S^1 is \mathbb{R} modulo 2π . For a fixed c ,

$$q_1 = c\psi_1^2 + \bar{c}\bar{\psi}_2^2 = c(\psi_1^+(q_0, \lambda_0))^2 + \bar{c}(\bar{\psi}_2^+(q_0, \lambda_0))^2$$

depends continuously on the location of λ_0 and the potential q_0 . Thus, the degree of the mapping $\bar{\theta}$ is unchanged under the multi-step isoperiodic deformation process. We can calculate its degree by substituting $k = -m/(jn)$ and $\lambda = -\text{sign}(m)\sqrt{k^2 + 1}$ into formula (22). Integrating that formula shows that

$$\text{Im} \log \left(c\psi_1^2 + \bar{c}\bar{\psi}_2^2 \right) = -\frac{i}{2} \log \left(\frac{u + (k + \lambda)^2 \bar{u}}{\bar{u} + (k + \lambda)^2 u} \right). \quad (23)$$

So, the period of $\arg(q_1)$ is $\pi/|k| = jn\pi/|m|$. Therefore, the degree of mapping $\bar{\theta}$ is m , taking the minus sign in (23) into account.

Because the curve $\delta^{-1}(\tilde{\gamma}(x))$ winds around the z -axis $|m|$ times (in a counterclockwise direction when $m > 0$ and clockwise when $m < 0$) we see that it is a (j, m) torus knot in $S^1 \times D^2$. Thus, the curve $\tilde{\gamma}(x)$ is a (j, m) cable about γ_0 .

5.5. Conclusions. We may now state our main result in full:

Theorem 5.1. *Let n, m_1, \dots, m_K be relatively prime with $|m_k| > n > 0$, and let $g_k = \text{gcd}(n, m_1, \dots, m_k)$. Let $(*)_k$ be the isoperiodic deformation system with variables α_ℓ, λ_j for $0 \leq \ell \leq K, 1 \leq j \leq 2K + 2$, controls $c_k = 1, c_\ell = 0$ for $\ell \neq k$, and with change of variable $\xi = \frac{1}{2}\epsilon^2$. Then:*

1. *For each k between 1 and K there exists $\rho_k > 0$ such that $(*)_k$ has analytic solution $(\alpha_\ell^{(k)}, \lambda_j^{(k)})$ for $|\epsilon| < \rho_k$ satisfying, when $k = 1$,*

$$\begin{aligned} \alpha_0^{(1)}(0) &= 0, \quad \lambda_1^{(1)}(0) = i, \quad \lambda_2^{(1)}(0) = -i, \quad \frac{d\lambda_3^{(k)}}{d\epsilon}(0) = -\frac{d\lambda_4^{(k)}}{d\epsilon}(0) = i, \\ \alpha_\ell^{(1)}(0) &= \lambda_{2\ell+1}^{(1)}(0) = \lambda_{2\ell+2}^{(1)}(0) = -\text{sign}(m_\ell)\sqrt{(m_\ell/n)^2 - 1}, \quad 1 \leq \ell \leq K. \end{aligned}$$

and when $k > 1$ (with ρ_k depending on the choice of $\epsilon_{k-1} \in (0, \rho_{k-1})$)

$$\alpha_\ell^{(k)}(0) = \alpha_\ell^{(k-1)}(\epsilon_{k-1}), \lambda_j^{(k)}(0) = \lambda_j^{(k-1)}(\epsilon_{k-1}), \frac{d\lambda_{2k+1}^{(k)}}{d\epsilon}(0) = -\frac{d\lambda_{2k+2}^{(k)}}{d\epsilon}(0) = i$$

2. *For each k there exist finite-gap potentials $q^{(k)}(x; \epsilon)$ which are $n\pi$ -periodic in x , analytic in ϵ , and for which the simple points are $\lambda_j^{(k)}(\epsilon), 1 \leq j \leq 2k + 2$. Then the filament $\gamma^{(k)}(x; \epsilon)$, constructed from $q^{(k)}$ using the Sym-Pohlmeyer formula at $\Lambda_0 = \alpha_0^{(k)}(\epsilon)$, is closed of length $\pi n/g_k$ and is a $(g_{k-1}/g_k, m_k/g_k)$ -cable about $\gamma^{(k)}(x; \epsilon_k)$.*

The argument given in Section 7 implies that for each k there is a deformation $q^{(k)}(x, t; \epsilon)$ of NLS solutions whose spectrum matches the deformation of the branch points at any time. The above theorem, applied at any fixed time t_0 , implies that the corresponding filament $\gamma^{(k)}(x, t_0; \epsilon_k)$ has the desired cable type. (Note that the plane wave potential $q^{(0)}$ at time t_0 only differs from that at time zero by multiplication by a unit modulus constant.) Thus, we have the

Corollary 5.2. *The knot type of $\gamma^{(k)}(x, t; \epsilon_k)$ is fixed for all time.*

The local nature of the VFE can, in general, cause the knot type to change in time. Indeed, it is relatively easy to construct solutions with changing knot type by taking Bäcklund transformations of genus one finite-gap solutions. Thus the Corollary implies that we can nonetheless construct a neighborhood of the multiply-covered circle, within the class of finite-gap VFE solutions, which consists of filaments whose knot is preserved.

6. APPENDIX: COMPLETENESS OF THE SQUARED EIGENFUNCTIONS

In this Appendix we summarize the main properties of squared eigenfunctions for the NLS equation, in particular their connection to the linearized NLS equation, their biorthogonality property, and the L^2 -completeness of a suitably chosen periodic subfamily.

We rewrite the NLS equation as a dynamical system

$$\begin{aligned} iq_t &= -q_{xx} + 2q^2r, \\ ir_t &= r_{xx} - 2r^2q, \end{aligned} \tag{24}$$

for the pair (q, r) in the phase space $\mathcal{P} = H_{per}^1([0, L], \mathbb{C}^2) \subset L^2([0, 1], \mathbb{C}^2)$ of periodic, square integrable, vector-valued functions of x , with square integrable first derivative. The inner product is taken to be the one of the ambient space:

$$\langle \mathbf{f}, \mathbf{g} \rangle = \frac{1}{L} \int_0^L [f_1(x)\bar{g}_1(x) + f_2(x)\bar{g}_2(x)] dx, \tag{25}$$

where $\mathbf{f} = (f_1, f_2)$, $\mathbf{g} = (g_1, g_2)$ are in \mathcal{P} .

The focusing/defocusing reality condition is achieved by restricting to one of the invariant subspaces $\mathcal{P}^\pm = \{(q, r) \in \mathcal{P} \mid r = \pm\bar{q}\}$ on which the inner product (25) becomes the real inner product

$$\langle \mathbf{f}, \mathbf{g} \rangle_R = \frac{2}{L} \operatorname{Re} \left(\int_0^L u(x)\bar{v}(x) dx \right),$$

where $\mathbf{f} = (u, \pm\bar{u})$, $\mathbf{g} = (v, \pm\bar{v})$ are elements of \mathcal{P}^\pm .

For a given NLS potential $\mathbf{q} = (q, r) \in \mathcal{P}$, we consider the linearization of the NLS system (24), obtained by replacing $q \rightarrow q + u$, $r \rightarrow r + v$ and retaining terms up to first order in u and v ,

$$\begin{aligned} iu_t + u_{xx} - 2q^2v - 4qru &= 0 \\ iv_t - v_{xx} + 2r^2u + 4qrv &= 0. \end{aligned} \tag{26}$$

For fixed time t_0 , we regard the pair (u, v) as an element of the ambient space $L^2([0, L], \mathbb{C}^2)$, endowed with Hermitian inner product given by (25).

6.1. Squared Eigenfunctions. If ϕ and $\tilde{\phi}$ are solutions of the NLS linear system (33) at the same value of λ , then the triplet

$$\phi \otimes \tilde{\phi} = \begin{bmatrix} \frac{1}{2}(\phi_1\tilde{\phi}_2 + \tilde{\phi}_1\phi_2) \\ \phi_1\tilde{\phi}_1 \\ -\phi_2\tilde{\phi}_2 \end{bmatrix} = \begin{bmatrix} f \\ g \\ h \end{bmatrix}, \tag{27}$$

solves the *squared eigenfunction* systems:

$$\begin{bmatrix} f \\ g \\ h \end{bmatrix}_x = \begin{pmatrix} 0 & -ir & -iq \\ 2iq & -2i\lambda & 0 \\ 2ir & 0 & 2i\lambda \end{pmatrix} \begin{bmatrix} f \\ g \\ h \end{bmatrix}. \quad (28)$$

$$\begin{bmatrix} f \\ g \\ h \end{bmatrix}_t = \begin{pmatrix} 0 & -(2i\lambda r + r_x) & -(2i\lambda q - q_x) \\ 2(2i\lambda q - q_x) & -2(2i\lambda^2 + iqr) & 0 \\ 2(2i\lambda r + r_x) & 0 & 2(2i\lambda^2 + iqr) \end{pmatrix} \begin{bmatrix} f \\ g \\ h \end{bmatrix}. \quad (29)$$

The following properties can be easily verified using systems (29), (28):

Proposition 6.1. (1) (linearization) The pair $(g, h) = (\phi_1 \tilde{\phi}_1, -\phi_2 \tilde{\phi}_2)$ solves the linearized NLS equations (26).

(2) (biorthogonality) Suppose that $\lambda \neq \mu$ are distinct points of the periodic/antiperiodic spectrum of the spatial linear operator $\mathcal{L}_1 = i\sigma_3 \frac{d}{dx} + \begin{pmatrix} 0 & q \\ r & 0 \end{pmatrix}$. Let $(g(\lambda), h(\lambda))$ and $(\tilde{g}(\mu), \tilde{h}(\mu))$ be solutions of the squared eigenfunction systems. Then,

$$\left\langle \begin{pmatrix} g(\lambda) \\ h(\lambda) \end{pmatrix}, J \overline{\begin{pmatrix} \tilde{g}(\mu) \\ \tilde{h}(\mu) \end{pmatrix}} \right\rangle = 0. \quad (30)$$

6.2. A basis of squared eigenfunctions. Given a finite-genus NLS potential q , one can construct a periodic subfamily of solutions of the linearized NLS equation which, for fixed t , is also a basis for $L^2([0, L], \mathbb{C}^2)$. Its elements are squared eigenfunctions constructed from Bloch eigenfunctions evaluated at a countable number of points of the spectrum of q .

The Bloch eigenfunctions are common solutions of the AKNS system and the shift operator, i.e., they satisfy the additional property

$$\varphi^\pm(x + L) = \rho^\pm(\lambda) \varphi^\pm(x),$$

where $\rho^\pm(\lambda)$ are the Floquet multipliers

$$\rho^\pm(\lambda) = \frac{\Delta(\lambda) \pm \sqrt{\Delta^2(\lambda) - 4}}{2}. \quad (31)$$

A useful normalization is obtained by selecting (see [23, 24])

$$\begin{aligned} \varphi^+ &= e^{i\frac{\pi}{4}} \sqrt{\frac{\rho^-(\lambda) - M_{11}(\lambda)}{M_{12}(\lambda)(\Delta^2(\lambda) - 4)}} [M_{12}(\lambda) \mathbf{Y}_1 + (\rho^+(\lambda) - M_{11}(\lambda)) \mathbf{Y}_2], \\ \varphi^- &= e^{i\frac{\pi}{4}} \sqrt{\frac{\rho^+(\lambda) - M_{11}(\lambda)}{M_{12}(\lambda)(\Delta^2(\lambda) - 4)}} [M_{12}(\lambda) \mathbf{Y}_1 + (\rho^-(\lambda) - M_{11}(\lambda)) \mathbf{Y}_2]. \end{aligned} \quad (32)$$

so as to satisfy the useful symmetry

$$\varphi^-(x; \lambda) = \overline{J \varphi^+(x; \bar{\lambda})}.$$

In the expressions above, $M_{ij}(\lambda)$ are the entries of the transfer matrix $M(x, t; \lambda) = \Phi(x + L, t; \lambda) \Phi(x, t; \lambda)^{-1}$ across a spatial period L , and the vectors \mathbf{Y}_i are the columns of the fundamental matrix solution of the AKNS system (26).

For simplicity, we consider an NLS potential (q, r) the critical points of which are of algebraic and geometric multiplicity two. (Higher order critical points introduce some technical difficulty, while critical points of geometric multiplicity one can be dealt with in a simple way.) We define the following family of squared eigenfunctions.

(A) At the real and complex double points $\{\lambda_j^d\}$:

$$\mathbf{f}^{(+,j)}(x) = \begin{pmatrix} (\varphi_1^+)^2(x; \lambda) \\ -(\varphi_2^+)^2(x; \lambda) \end{pmatrix}_{\lambda=\lambda_j^d}, \quad \mathbf{f}^{(-,j)} = \begin{pmatrix} (\varphi_1^-)^2(x; \lambda) \\ -(\varphi_2^-)^2(x; \lambda) \end{pmatrix}_{\lambda=\lambda_j^d}.$$

(B) At the finite number N of critical points $\{\lambda_k^c\}$ that are not elements of the periodic/antiperiodic spectrum of q :

$$\mathbf{f}^{(c,k)} = \begin{pmatrix} (\varphi_1^+ \varphi_1^-)(x; \lambda) \\ -(\varphi_2^+ \varphi_2^-)(x; \lambda) \end{pmatrix}_{\lambda=\lambda_k^c},$$

(C) At N (appropriately selected) simple points $\{\lambda_i^s\}$ of the spectrum (half the number of branch points of the associated Riemann surface):

$$\mathbf{f}^{(s,i)} = \begin{pmatrix} (\varphi_1^+)^2(x; \lambda) \\ -(\varphi_2^+)^2(x; \lambda) \end{pmatrix}_{\lambda=\lambda_{2i}^s}, \quad k, i = 1, \dots, N.$$

Then

Theorem 6.2 (Completeness). *The family*

$$\{\mathbf{f}^{(+,j)}, \mathbf{f}^{(-,j)}\}_{\lambda_j^d} \cup \{\mathbf{f}^{(c,k)}\}_{\lambda_k^c} \cup \{\mathbf{f}^{(s,i)}\}_{\lambda_i^s}$$

is a basis of $L^2([0, L], \mathbb{C}^2)$.

A proof of this fact can be found in the preprint [7], following the roadmap developed in [9] for the sine-Gordon equation and incorporating ideas from [20]. We also mention the following result:

Lemma 6.3 (Biorthogonal Pairing). *The families $\{\mathbf{f}^{(+,j)}\}$ and $\{J\overline{\mathbf{f}}^{(-,k)}\}$; $\{\mathbf{f}^{(-,j)}\}_{|j|>N}$ and $\{J\overline{\mathbf{f}}^{(+,k)}\}$, are biorthogonally paired with respect to the Hilbert space inner product (25):*

$$\langle \mathbf{f}^{(\pm,j)}, J\overline{\mathbf{f}}^{(\mp,k)} \rangle = C_j \delta_{jk},$$

where $C_j = \frac{1}{2i} \sqrt{\Delta(\lambda_j) \Delta''(\lambda_j)} (W[\varphi^+(x; \lambda_j), \varphi^-(x; \lambda_j)])^2$.

Notice that the existence of a biorthogonal pairing automatically guarantees that the family of squared eigenfunctions evaluated at the double points of the spectrum of q form a linearly independent set.

7. APPENDIX: ANALYTIC DEPENDENCE OF THE POTENTIAL ON THE DEFORMATION PARAMETER

The reconstruction of a finite-gap potential of genus g relies on choice of $2g + 2$ branch points in the complex plane and also on a choice of an effective divisor \mathcal{D} of degree $g + 1$ (satisfying a certain reality condition) on the hyperelliptic Riemann surface defined by the branch points. Thus, to specify an isoperiodic deformation of the NLS potential q we must specify not only a deformation of the branch points but also a deformation of the divisor (or an equivalent set of auxiliary data). In this appendix, we show that, at the same time that a double point is being opened up by homotopic deformation, the auxiliary data given by the Dirichlet spectrum may be deformed in a way that guarantees that q is analytic in the deformation parameter ϵ . This result is necessary for us to carry out the perturbation expansions in §4 and §5.

7.1. Finite-Gap Solutions and the Dirichlet Spectrum. The Dirichlet spectrum of an NLS solution $q(x, t)$ which is L -periodic in x is defined as follows (see [1], [24]). Given a fundamental matrix solution Φ for the AKNS system

$$\phi_x = \begin{pmatrix} -i\lambda & iq \\ i\bar{q} & i\lambda \end{pmatrix} \phi, \quad \phi_t = \begin{pmatrix} i(|q|^2 - 2\lambda^2) & 2i\lambda q - q_x \\ 2i\lambda\bar{q} + \bar{q}_x & -i(|q|^2 - 2\lambda^2) \end{pmatrix} \phi, \quad (33)$$

we construct the transfer matrix

$$M(x, t; \lambda) = \Phi(x + L, t; \lambda)\Phi(x, t; \lambda)^{-1},$$

There are two sets of Dirichlet eigenvalues:

- The Dirichlet eigenvalues $\mu_k(x, t)$ are the λ -values for which

$$M_{11} - M_{22} + M_{12} - M_{21} = 0. \quad (34)$$

Equivalently, these are the values for which there is a nontrivial solution of (33) satisfying the boundary condition $\phi_1 + \phi_2 = 0$ at (x, t) and at $(x + L, t)$.

- The Dirichlet eigenvalues $\nu_k(x, t)$ are the λ -values for which

$$M_{11} - M_{22} - i(M_{12} + M_{21}) = 0.$$

Equivalently, these are the values for which there is a nontrivial solution of (33) satisfying $i\phi_1 + \phi_2 = 0$ at (x, t) and $(x + L, t)$. Also, these are the μ -eigenvalues that result when q is replaced by iq .

The μ_k and ν_k are dependent on x and t , satisfying a system of ODEs first derived by Ablowitz and Ma [1]. However, for finite-gap solutions, all but finitely many of each set are locked to the double points of the Floquet spectrum. (This is true more generally for periodic NLS potentials whose Sobolev norm over one period is bounded; see [24].)

In order to get the equations defining the Dirichlet eigenvalues, we need to use the formulas for finite-gap NLS solutions and their associated Baker eigenfunction. We will briefly review their construction; further details are available in the book [2] or our paper [6].

One starts with a hyperelliptic Riemann surface Σ defined by

$$\zeta^2 = \prod_{j=1}^{2g+2} (\lambda - \lambda_j), \quad (35)$$

where the branch points λ_j occur in complex conjugate pairs. This surface is compactified by the points ∞_{\pm} , where $\lambda^{g+1}/\zeta \rightarrow \pm 1$. After selecting a suitable homology basis a_j, b_j (see Figure 5), one constructs holomorphic differentials ω_j such that $\oint_{a_k} \omega_j = 2\pi i \delta_{jk}$ and meromorphic differentials $d\Omega_1, d\Omega_2, d\Omega_3$ with prescribed singularities at ∞_{\pm} and zero a -periods. Then

$$q(x, t) = A \exp(-iEx + iNt) \frac{\theta(i\mathbf{V}x + i\mathbf{W}t - \mathbf{D} - \mathbf{r})}{\theta(i\mathbf{V}x + i\mathbf{W}t - \mathbf{D})}, \quad (36)$$

where

- $\theta : \mathbb{C}^g \rightarrow \mathbb{C}$ is the Riemann theta function, with period lattice generated by the vectors $2\pi i \mathbf{e}_j$ (where $\{\mathbf{e}_j\}$ is the standard basis of unit vectors) and with quasiperiods given by the columns of the Riemann matrix B defined by $B_{jk} = \oint_{b_k} \omega_j$;
- \mathbf{V}, \mathbf{W} , and $-\mathbf{r}$ are the vectors of b -periods of $d\Omega_1, d\Omega_2, d\Omega_3$ respectively;

- the Abelian integrals $\Omega_1, \Omega_2, \Omega_3$, with the branch point λ_{2g+2} in the lower half-plane as basepoint, have asymptotic behavior

$$\begin{aligned}\Omega_1(P) &\sim \pm \left(\lambda - \frac{E}{2} + o(1) \right), \\ \Omega_2(P) &\sim \pm \left(2\lambda^2 + \frac{N}{2} + o(1) \right), \\ \exp(\Omega_3(P)) &\sim \pm \left(\frac{2i}{A}\lambda + o(1) \right)\end{aligned}$$

as $P \rightarrow \infty_{\pm}$, where A is real and positive. (Because they have nonzero b -periods, the integrals are not well-defined on Σ , but are well-defined on the surface Σ_0 obtained after cutting Σ along the homology basis.)

- The vector \mathbf{D} is defined so that the zero divisor of $\theta(\mathcal{A}(P) - \mathbf{D})$ is the positive divisor \mathcal{D}_+ linearly equivalent to $\mathcal{D} - \infty_+$, where \mathcal{A} is the Abel map defined by

$$\mathcal{A}(P) = \int_{\infty_-}^P \boldsymbol{\omega}$$

and $\boldsymbol{\omega}$ is the vector of holomorphic differentials ω^j . (The reality condition on \mathcal{D} is that \mathbf{D} have zero real part.)

A vector solution of (33) is provided at each $P \in \Sigma$ by the Baker eigenfunction $\boldsymbol{\psi}$, with components

$$\psi_1(x, t) = \frac{\exp(i(\Omega_1(P)x + \Omega_2(P)t)) \theta(\mathcal{A}(P) + i\mathbf{V}x + i\mathbf{W}t - \mathbf{D})\theta(\mathbf{D})}{\exp(i(Ex - Nt)/2) \theta(i\mathbf{V}x + i\mathbf{W}t - \mathbf{D})\theta(\mathcal{A}(P) - \mathbf{D})}$$

and

$$\psi_2(x, t) = -i \frac{\exp(i(\Omega_1(P)x + \Omega_2(P)t) + \Omega_3(P)) \theta(\mathcal{A}(P) + i\mathbf{V}x + i\mathbf{W}t - \mathbf{D} - \mathbf{r})\theta(\mathbf{D})}{\exp(i(Nt - Ex)/2) \theta(i\mathbf{V}x + i\mathbf{W}t - \mathbf{D})\theta(\mathcal{A}(P) - \mathbf{D})}.$$

Although $\mathcal{A}(P)$ and $\Omega_i(P)$ are not well-defined on Σ because of nontrivial periods, we make the convention that the paths of integration for $\mathcal{A}(P)$ and $\Omega_i(P)$ differ by a fixed path from ∞_- to λ_{2g+2} in the cut surface Σ_0 , and this makes the Baker eigenfunction well-defined. (The rightmost theta-factors in the numerator and denominator, which were unfortunately omitted in [6], are necessary for this.)

Let $\iota : (\lambda, \zeta) \mapsto (\lambda, -\zeta)$ be the sheet interchange involution of the Riemann surface. When P is not a branch point, the Baker eigenfunctions $\boldsymbol{\psi}(P)$ and $\boldsymbol{\psi}(\iota P)$ are a basis for solutions of (33). Thus, to compute the initial values $\mu_k(0, 0)$ and $\nu_k(0, 0)$ of the Dirichlet spectrum, we evaluate $\boldsymbol{\psi}$ when $t = 0$ and $x = 0$ or $x = L$. Using the facts that $L\mathbf{V}/(2\pi)$ and $LE/(2\pi)$ are integer-valued, we get

$$\begin{aligned}\psi_1(0, 0) &= 1, & \psi_2(0, 0) &= -if(P), \\ \psi_1(L, 0) &= \exp\left(iL\left(\Omega_1(P) - \frac{E}{2}\right)\right), & \psi_2(L, 0) &= -if(P)\psi_1(L, 0),\end{aligned}$$

where

$$f(P) = \exp(\Omega_3(P)) \frac{\theta(\mathcal{A}(P) - \mathbf{D} - \mathbf{r})}{\theta(\mathcal{A}(P) - \mathbf{D})}.$$

So, $\psi_1 + \psi_2 = 0$ is satisfied at both ends if and only either $\sin(L\Omega_1(P)) = 0$ or $f(P) = -i$. This reflects the fact that every double point of the Floquet spectrum is a Dirichlet eigenvalue

which is constant in x and t . On the other hand, the function $f(P)$ is well-defined and meromorphic on Σ , with pole divisor $\mathcal{D}_+ + \infty_+$, so there are $g + 1$ Dirichlet eigenvalues $\mu_k(0, 0)$ that are not locked to the double points, and are located at the images of the points where $f(P) = -i$ under the projection $\pi : \Sigma \rightarrow \mathbb{C}$ onto the complex λ -plane. Similarly, the $\nu_k(0, 0)$ are either locked to double points or are images of the $g + 1$ points where $f(P) = 1$ when $x = t = 0$.

7.2. Deformations maintaining $\mathbf{D} = 0$.

Proposition 7.1. *When $\mathbf{D} = 0$, the points where $f(P) = 1$ (and hence the locations of $\nu_k(0, 0)$) are λ_{2g+2} and the branch points in the upper half plane (excluding $\overline{\lambda_{2g+2}}$). At the other branch points, $f(P) = -1$.*

Before sketching the proof, we note that in order for the ν -eigenvalues to deform continuously when further double points are opened up, the basepoint λ_{2g+2} must change continuously. Thus, we cannot take the convention (which we used in [6]) that it be located at the rightmost branch point in the lower half plane. Instead, we will keep it located at the branch point in the lower half plane that was originally part of the plane wave spectrum, located on the negative imaginary axis. Because this basepoint must be in the interior of the cut Riemann surface, we must rearrange our homology basis so that its cycles do not enclose this basepoint. (The extra cycle a_0 in the following diagram is not part of the homology basis.)

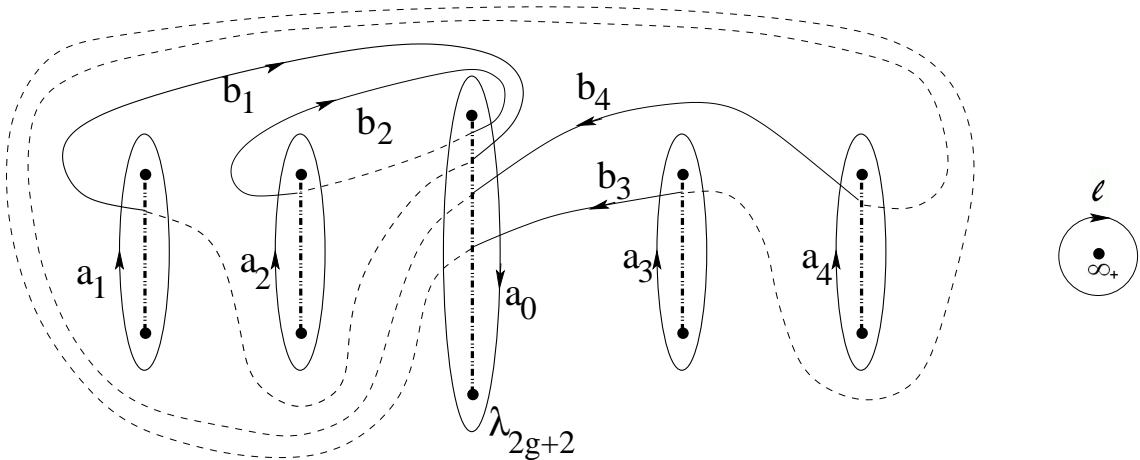


FIGURE 5. Homology basis adapted to isoperiodic deformations, for genus $g = 4$. Branch cuts extend between complex conjugate branch points; solid paths lie on the upper sheet, dashed on the lower sheet; basepoint for Abelian differentials $\Omega_1, \Omega_2, \Omega_3$ is marked as λ_{2g+2} . The extra cycles a_0 and ℓ are used in the proof below.

Proof. Because λ_{2g+2} is the basepoint for Ω_3 and $\mathcal{A}(\lambda_{2g+2}) = \mathbf{r}/2$, $f(\lambda_{2g+2}) = 1$. Let $\lambda_{2g+1} = \overline{\lambda_{2g+2}}$ in the upper half plane, and fix an integration path from λ_{2g+2} to λ_{2g+1} on the upper sheet on the right side of the branch cut. Because $d\Omega_3$ is a linear combination of differentials of the form $(\lambda^k/\zeta)d\lambda$, then $\Omega_3(\lambda_{2g+1}) = -\frac{1}{2} \oint_{a_0} d\Omega_3$. Furthermore, because $a_0 + a_1 + \dots + a_g$ is homologous to $-\ell$ in the surface Σ with the points ∞_{\pm} removed, then using the residue of $d\Omega_3$ at ∞_+ we get $\Omega_3(\lambda_{2g+1}) = \frac{1}{2} \oint_{\ell} d\Omega_3 = \pi i$. Similarly,

$$\mathcal{A}(\lambda_{2g+1}) = \mathcal{A}(\lambda_{2g+2}) - \frac{1}{2} \oint_{a_0} \omega = \frac{1}{2} \mathbf{r} + \pi i \mathbf{1}.$$

where $\boldsymbol{\omega}$ is the vector of normalized holomorphic differentials ω_k , and $\mathbf{1}$ is the vector whose entries are all equal to 1. Then, using the even-ness and periodicity of θ ,

$$f(\lambda_{2g+1}) = \exp(\pi i) \frac{\theta(\mathcal{A}(\lambda_{2g+1}) - \mathbf{r})}{\theta(\mathcal{A}(\lambda_{2g+1}))} = -\frac{\theta(\pi i \mathbf{1} - \frac{1}{2} \mathbf{r})}{\theta(\pi i \mathbf{1} + \frac{1}{2} \mathbf{r})} = -\frac{\theta(\frac{1}{2} \mathbf{r} - \pi i \mathbf{1})}{\theta(\pi i \mathbf{1} + \frac{1}{2} \mathbf{r})} = -1.$$

Suppose $\operatorname{Re}(\lambda_{2k-1}) < \operatorname{Re}(\lambda_{2g+2})$ and $\operatorname{Im}(\lambda_{2k-1}) > 0$. Let \tilde{b}_k be the cycle that runs from λ_{2k-1} to λ_{2g+1} along the upper sheet, and back along the same path along the lower sheet, whose projection to the λ -plane encircles no other branch points. Then $\tilde{b}_k \sim b_k + \sum a_m$, where the sum is over the a -cycles around branch cuts whose real part is strictly between that of λ_{2k-1} and λ_{2g+1} . Letting the path of integration from λ_{2g+2} to λ_{2g+1} be continued by the part of \tilde{b}_k on the lower sheet,

$$\Omega_3(\lambda_{2k-1}) = \Omega_3(\lambda_{2g+1}) + \frac{1}{2} \oint_{\tilde{b}_k} d\Omega_3 = \pi i - \frac{1}{2} r_k$$

and

$$\mathcal{A}(\lambda_{2k-1}) = \mathcal{A}(\lambda_{2g+1}) + \frac{1}{2} \oint_{\tilde{b}_k} d\Omega_3 = \frac{1}{2}(\mathbf{r} + B_k) + \pi i(\mathbf{1} + \sum \mathbf{e}_m),$$

where B_k indicates the k th column of the Riemann matrix. Then using evenness and periodicity of θ ,

$$\frac{\theta(\mathcal{A}(\lambda_{2k-1}) - \mathbf{r})}{\theta(\mathcal{A}(\lambda_{2k-1}))} = \frac{\theta(\frac{1}{2}(-\mathbf{r} + B_k) + \pi i(\mathbf{1} + \sum \mathbf{e}_m))}{\theta(\frac{1}{2}(\mathbf{r} + B_k) + \pi i(\mathbf{1} + \sum \mathbf{e}_m))} = \frac{\theta(\frac{1}{2}(\mathbf{r} - B_k) + \pi i(\mathbf{1} + \sum \mathbf{e}_m))}{\theta(\frac{1}{2}(\mathbf{r} - B_k) + \pi i(\mathbf{1} + \sum \mathbf{e}_m) + B_k)}.$$

Using the quasiperiodicity property $\theta(\mathbf{z} + B_k) = \exp(-z_k - \frac{1}{2} B_{kk}) \theta(\mathbf{z})$,

$$f(\lambda_{2k-1}) = \frac{\exp(\pi i - \frac{1}{2} r_k) \theta(\frac{1}{2}(\mathbf{r} - B_k) + \pi i(\mathbf{1} + \sum \mathbf{e}_m))}{\exp(-\frac{1}{2}(r_k - B_{kk}) + \pi i - \frac{1}{2} B_{kk}) \theta(\frac{1}{2}(\mathbf{r} - B_k) + \pi i(\mathbf{1} + \sum \mathbf{e}_m))} = 1.$$

Let $\lambda_{2k} = \overline{\lambda_{2k-1}}$ in the lower half-plane, and let the path from λ_{2g+2} to λ_{2k-1} be continued by the part of a_k to the left of the branch cut. Then $\Omega_3(\lambda_{2k}) = \Omega_3(\lambda_{2k-1}) - \frac{1}{2} \oint_{a_k} d\Omega_3 = \Omega_3(\lambda_{2k-1})$ and $\mathcal{A}(\lambda_{2k}) = \mathcal{A}(\lambda_{2k-1}) - \pi i \mathbf{e}_k$. Using evenness and periodicity,

$$\frac{\theta(\mathcal{A}(\lambda_{2k}) - \mathbf{r})}{\theta(\mathcal{A}(\lambda_{2k}))} = \frac{\theta(\frac{1}{2}(-\mathbf{r} + B_k) + \pi i(\mathbf{1} - \mathbf{e}_k + \sum \mathbf{e}_m))}{\theta(\frac{1}{2}(\mathbf{r} + B_k) + \pi i(\mathbf{1} - \mathbf{e}_k + \sum \mathbf{e}_m))} = \frac{\theta(\frac{1}{2}(\mathbf{r} - B_k) + \pi i(\mathbf{1} - \mathbf{e}_k + \sum \mathbf{e}_m))}{\theta(\frac{1}{2}(\mathbf{r} - B_k) + \pi i(\mathbf{1} - \mathbf{e}_k + \sum \mathbf{e}_m) + B_k)}.$$

Then, using quasiperiodicity,

$$f(\lambda_{2k}) = \frac{\exp(\pi i - \frac{1}{2} r_k) \theta(\frac{1}{2}(\mathbf{r} - B_k) + \pi i(\mathbf{1} - \mathbf{e}_k + \sum \mathbf{e}_m))}{\exp(-\frac{1}{2}(r_k - B_{kk}) - \frac{1}{2} B_{kk}) \theta(\frac{1}{2}(\mathbf{r} - B_k) + \pi i(\mathbf{1} - \mathbf{e}_k + \sum \mathbf{e}_m))} = -1.$$

Similarly, assuming that $\operatorname{Re}(\lambda_{2k-1}) > \operatorname{Re}(\lambda_{2g+1})$, $\operatorname{Im}(\lambda_{2k-1}) > 0$ and $\lambda_{2k} = \overline{\lambda_{2k-1}}$, we calculate that $f(\lambda_{2k-1}) = 1$ and $f(\lambda_{2k}) = 1$. \square

Proposition 7.1 implies that, if we maintain the choice $\mathbf{D} = 0$, any deformation of the branch points that is analytic in parameter ϵ will induce an analytic deformation of the initial values $\nu_k(0, 0)$. This is also true if we increase the genus by analytically splitting a double point of the Floquet spectrum at $\epsilon = 0$ into two branch points for $\epsilon \neq 0$, since the extra ν -eigenvalue that is unlocked at the higher genus still belongs to the Dirichlet spectrum as it limits to a double point when $\epsilon = 0$. It is also true for the isoperiodic deformations described in §2 that any other double point deforms analytically in ϵ , and so any locked Dirichlet eigenvalues are analytic in ϵ .

The μ -eigenvalues also deform analytically in ϵ . For, when $\mathbf{D} = 0$, the function f satisfies $f(\iota P) = 1/f(P)$. Thus,

$$h(\lambda) = f(P) + f(P)^{-1}, \quad \lambda = \pi(P)$$

is a well-defined meromorphic function on the complex plane with pole divisor $\pi(D_+ + \infty_+)$. The zeros of this function are $\mu_k(0, 0)$, so it has the form

$$h(\lambda) = \frac{\prod_{k=0}^g (\lambda - \mu_k(0, 0))}{r(\lambda)},$$

where $r(\lambda)$ is a polynomial of degree g . At each branch point $h(\lambda) = \pm 2$; the $\nu_k(0, 0)$ are zeros of $h(\lambda) - 2$, while the remaining branch points are zeros of $h(\lambda) + 2$. Because the coefficients of the polynomials in the numerator of $h(\lambda) \pm 2$ must be analytic in ϵ , it follows that the coefficients of the numerator of $h(\lambda)$ are analytic in ϵ . Then the $\mu_k(0, 0)$ are analytic in ϵ so long as they are distinct; however, distinctness holds for sufficiently small ϵ at each deformation step.

7.3. Trace Formulas. The NLS solution $q(x, t)$ is determined by the Dirichlet spectrum and branch points by the trace formulas⁴

$$\begin{aligned} q(x, t) + r(x, t) &= \sum_{k=0}^g (\lambda_{2k} + \lambda_{2k-1} - 2\mu_k(x, t)) \\ q(x, t) - r(x, t) &= -i \sum_{k=0}^g (\lambda_{2k} + \lambda_{2k-1} - 2\nu_k(x, t)), \end{aligned}$$

where we take the specialization $r = -\bar{q}$ for the focusing case.

Given the branch points and the initial values $\mu_k(0, 0)$ and $\nu_k(0, 0)$, the values of $\mu_k(x, t)$ and $\nu_k(x, t)$ are determined by ODE systems derived by Ablowitz and Ma [1]:

$$\begin{aligned} \frac{\partial \mu_k}{\partial x} &= \frac{i\zeta(\mu_k) \left(c - \sum_{j \neq k} \mu_j \right)}{\prod_{j \neq k} (\mu_j - \mu_k)}, \\ \frac{\partial \mu_k}{\partial t} &= 2\mu_k \frac{\partial \mu_k}{\partial x} + \frac{2i\zeta(\mu_k)}{\prod_{j \neq k} (\mu_j - \mu_k)} \left[\left(\frac{c}{2} - \sum_{j=0}^g \mu_j \right)^2 + \left(\frac{c}{2} - \sum_{j=0}^g \nu_j \right)^2 - \sum_{j=0}^g \frac{\partial \nu_j}{\partial x} \right], \end{aligned}$$

where $c = \sum_{m=1}^{2g+2} \lambda_m$, and

$$\begin{aligned} \frac{\partial \nu_k}{\partial x} &= \frac{i\zeta(\nu_k) \left(c - \sum_{j \neq k} \nu_j \right)}{\prod_{j \neq k} (\nu_j - \nu_k)}, \\ \frac{\partial \nu_k}{\partial t} &= 2\nu_k \frac{\partial \nu_k}{\partial x} + \frac{2i\zeta(\nu_k)}{\prod_{j \neq k} (\nu_j - \nu_k)} \left[\left(\frac{c}{2} - \sum_{j=0}^g \mu_j \right)^2 + \left(\frac{c}{2} - \sum_{j=0}^g \nu_j \right)^2 - \sum_{j=0}^g \frac{\partial \mu_j}{\partial x} \right]. \end{aligned}$$

In these systems, the branch points λ_m and initial values $\mu_k(0, 0)$, $\nu_k(0, 0)$ depend analytically on ϵ . Our choice $\mathbf{D} = 0$ implies that the initial values $\nu_k(0, 0)$ are located at branch points, where $\zeta = 0$. Thus, the ν_k are constant in x and t , and are automatically analytic in ϵ .

⁴These are adapted from [24], after making the changes $q \mapsto -2q$, $r \mapsto -2r$, $\lambda \mapsto -\lambda$ which are necessary to make their version of NLS and its Lax pair coincide with ours.

In the system for the μ_k , $\zeta(\mu_k)$ is to be evaluated along the upper sheet. (According to [11], the μ -eigenvalues travel along the a -cycles of the Riemann surface.) Note that when $\epsilon = 0$, the initial values of one of the μ -eigenvalues is a double point, the limit of two complex conjugate branch points that coalesce as $\epsilon \rightarrow 0$. The above characterization of the $\mu_k(0, 0)$ as points where $f(P) = -i$, coupled with the fact that $f(\tau P) = -\overline{f(P)}$ ensures that the $\mu_k(0, 0)$ lie along the real axis. Thus, each $\zeta(\mu_k(0, 0))$ will be analytic in ϵ , including at $\epsilon = 0$.

It follows that the $\mu_k(x, t)$ and $\nu_k(x, t)$ are analytic in ϵ for any x and t . Then the trace formulas imply that $q(x, t)$ is analytic in ϵ .

REFERENCES

- [1] Ablowitz M. and Ma, Y., *The Periodic Cubic Schrödinger Equation*, Stud. Appl. Math. **65** (1981), 113–158.
- [2] Belokolos E., Bobenko A., Enolskii A. B. V., Its A., and Matveev V., *Algebro-Geometric Approach to Nonlinear Integrable Equations*, Springer, 1994.
- [3] Calini A., *Recent developments in integrable curve dynamics*, in *Geometric Approaches to Differential Equations*, Austral. Math. Soc. Lect. Ser., **15**, Cambridge University Press (2000), 56–99.
- [4] Calini A. and Ivey T., *Bäcklund transformations and knots of constant torsion*, J. Knot Theory Ramif. **7** (1998), 719–746.
- [5] ———, *Connecting geometry, topology and spectra for finite-gap NLS potentials*, Physica D **152/153** (2001), 9–19.
- [6] ———, *Finite-gap Solutions of the Vortex Filament Equation: Genus One Solutions and Symmetric Solutions* J. Nonlinear Sci., **15** (2005) no. 5, 321–361.
- [7] Calini A. and Ercolani N. M., *Completeness of the squared eigenfunctions for the focussing NLS equation*, in preparation (2006).
- [8] Cieśliński J. and Gragert P. K. H. and Sym A. *Exact solution to localized-induction-approximation equation modeling smoke ring motion*, Phys. Rev. Lett. **57** (1986), 1507–1510.
- [9] Ercolani N. M., Forest, M. G. and McLaughlin D. W., *Geometry of the modulational instability, I: Local analysis*. unpublished draft, 1987.
- [10] Flaschka H., Forest M. G., and McLaughlin D. W. *Multiphase averaging and the inverse spectral solution of the KdV equation*. Comm. Pure Appl. Math. **33** (1980), 739–784.
- [11] Forest M. G. and Lee J. E., *Geometry and modulation theory for the periodic Schrödinger equation*, in *Oscillation Theory, Computation, and Methods of Compensated Compactness*. IMA in Math and Its Applications **2**, Dafermos et al. Editors, Springer-Verlag, New York (1986), 35–70.
- [12] Faddeev L. D. and Takhtajan L. A., *Hamiltonian Methods in the Theory of Solitons*, Springer, 1980.
- [13] Grinevich P. G., *Approximation theorem for the self-focusing nonlinear schrödinger equation and for the periodic curves in \mathbb{R}^3* , Physica D **152/153** (2001), 20–27.
- [14] Grinevich P. G. and Schmidt M. U. *Period preserving nonisospectral flows and the moduli space of periodic solutions of soliton equations: the nonlinear Schrödinger equation*. Phys. D **87** (1995), 73–98.
- [15] ———, *Closed curves in \mathbb{R}^3 : a characterization in terms of curvature and torsion, the hasimoto map and periodic solutions of the filament equation*, (1997). SFB 288 preprint no. 254, and dg-ga/9703020.
- [16] Hasimoto R., *A soliton on a vortex filament*, J. Fluid Mech. **51** (1972), 477–485.
- [17] Ivey T. and Singer D., *Knot types, homotopies and stability of closed elastic rods*, Proc. London Math. Soc. **79** (1999), 429–450.
- [18] Iwano M., *Local Theory of Nonlinear Differential Equations*, pp. 17-38 in *Analytic Theory of Ordinary Differential Equations*, Recent Prog. Nat. Sci. Japan **1** (1976), 1–55.
- [19] Keener, J. P., *Knotted vortex filaments in an ideal fluid*, J. Fluid Mech. **211** (1990), 629–651.
- [20] Krichever I. M. *Perturbation in periodic problems for two-dimensional integrable systems*. Sov. Sci. Rev. C. Math. Phys. **9** (1992), 1–103.
- [21] ———, *The τ -function of the universal Whitham hierarchy, matrix models and topological field theories*. Comm. Pure Appl. Math. **47** (1994) no. 4, 437-475.
- [22] Langer J. and Perline R., *Poisson geometry of the filament equation*, J. Nonlinear Sci. **1** (1991), 71–93.
- [23] Li Y. and McLaughlin D., *Morse and Melnikov functions for NLS Pde's*, Commun. Math. Phys., **162** (1994), 175–214.

- [24] McLaughlin D. W. and Overman E. A II. *Whiskered Tori for Integrable Pde's: Chaotic Behavior in Integrable Pde's.* in Surveys in Applied Mathematics **1**, Plenum Press (1995), 83–203.
- [25] Pohl W, *The Self-Linking Number of a Closed Space Curve*, Journal of Math. & Mech. **17** (1968), 975–985.
- [26] Pohlmeyer K., *Integrable hamiltonian systems and interactions through quadratic constraints*, Comm. Math. Phys. **46** (1976), 207–221.
- [27] Sasaki N. *Differential geometry and integrability of the Hamiltonian system of a closed vortex filament*, Lett. Math. Phys. **39** (1997) no. 3, 229–241.
- [28] Schmidt M. U. *Integrable systems and Riemann surfaces of infinite genus*, Memoirs of the American Mathematical Society, **551** (1996).
- [29] Sym A., *Soliton surfaces II*, Lettere al Nuovo Cimento **36** (1983), 307–312.
- [30] ———, *Vortex filament motion in terms of Jacobi theta functions*, Fluid Dynamics Research **3** (1988), 151–156.
- [31] White J., *Self-linking and the Gauss integral in higher dimensions*, Am. J. Math **91** (1969), 693–728.
- [32] Zakharov V. and Shabat A. B., *Exact theory of the 2-d self-focusing and the 1-d self-modulation in nonlinear media*, Soviet Phys. JETP **34** (1972), 62–69.
- [33] Zubov V. I., *Methods of A.M. Lyapunov and Their Application*, Noordhoff, 1964 [English translation; orig. publ. Izdat. Leningrad University, Moscow, 1957].

DEPARTMENT OF MATHEMATICS, COLLEGE OF CHARLESTON, CHARLESTON SC 29424 USA
E-mail address: calinia@cofc.edu, iveyt@cofc.edu